



Article

Proteome and Interactome Linked to Metabolism, Genetic Information Processing, and Abiotic Stress in Gametophytes of Two Woodferns

Sara Ojosnegros¹, José Manuel Alvarez¹ , Jonas Grossmann^{2,3}, Valeria Gagliardini⁴, Luis G. Quintanilla⁵ , Ueli Grossniklaus⁴ and Helena Fernández^{1,*}

- ¹ Area of Plant Physiology, Department of Organisms and Systems Biology, University of Oviedo, 33071 Oviedo, Spain; uo286037@uniovi.es (S.O.); alvarezmanuel@uniovi.es (J.M.A.)
² Functional Genomic Center Zurich, University and ETH Zurich, 8092 Zurich, Switzerland; jg@fgcz.ethz.ch
³ Swiss Institute of Bioinformatics, 1015 Lausanne, Switzerland
⁴ Department of Plant and Microbial Biology & Zurich-Basel Plant Science Center, University of Zurich, 8008 Zurich, Switzerland; vgagliar@botinst.uzh.ch (V.G.); grossnik@botinst.uzh.ch (U.G.)
⁵ Department of Biology and Geology, Physics and Inorganic Chemistry, University Rey Juan Carlos, 28933 Móstoles, Spain; luis.quintanilla@urjc.es
* Correspondence: fernandezelena@uniovi.es; Tel.: +34-985-104-811

Abstract: Ferns and lycophytes have received scant molecular attention in comparison to angiosperms. The advent of high-throughput technologies allowed an advance towards a greater knowledge of their elusive genomes. In this work, proteomic analyses of heart-shaped gametophytes of two ferns were performed: the apomictic *Dryopteris affinis* ssp. *affinis* and its sexual relative *Dryopteris oreades*. In total, a set of 218 proteins shared by these two gametophytes were analyzed using the STRING database, and their proteome associated with metabolism, genetic information processing, and responses to abiotic stress is discussed. Specifically, we report proteins involved in the metabolism of carbohydrates, lipids, and nucleotides, the biosynthesis of amino acids and secondary compounds, energy, oxide-reduction, transcription, translation, protein folding, sorting and degradation, and responses to abiotic stresses. The interactome of this set of proteins represents a total network composed of 218 nodes and 1792 interactions, obtained mostly from databases and text mining. The interactions among the identified proteins of the ferns *D. affinis* and *D. oreades*, together with the description of their biological functions, might contribute to a better understanding of the function and development of ferns as well as fill knowledge gaps in plant evolution.

Keywords: *Dryopteris affinis* ssp. *affinis*; *Dryopteris oreades*; fern; gametophyte; non-seed plant; proteome; STRING database



Citation: Ojosnegros, S.; Alvarez, J.M.; Grossmann, J.; Gagliardini, V.; Quintanilla, L.G.; Grossniklaus, U.; Fernández, H. Proteome and Interactome Linked to Metabolism, Genetic Information Processing, and Abiotic Stress in Gametophytes of Two Woodferns. *Int. J. Mol. Sci.* **2023**, *24*, 12429. <https://doi.org/10.3390/ijms241512429>

Academic Editor: Setsuko Komatsu

Received: 23 June 2023

Revised: 27 July 2023

Accepted: 31 July 2023

Published: 4 August 2023



Copyright: © 2023 by the authors. Licensee MDPI, Basel, Switzerland. This article is an open access article distributed under the terms and conditions of the Creative Commons Attribution (CC BY) license (<https://creativecommons.org/licenses/by/4.0/>).

1. Introduction

Ferns and lycophytes represent a genetic legacy of great value, being descendants of the first plants that evolved vascular tissues about 470 million years ago. They are distributed throughout the world and play an important role in ecosystem functioning. Compared to angiosperms, they have received scant attention, relegating them to the background after a splendid past. The aesthetic appeal of their leaves and their use to alleviate ailments in traditional medicine is all that these plant groups have traditionally inspired. Specifically, fern gametophytes are ideal organisms for research on plant growth and reproduction, which is facilitated by a simple in vitro culture system and their small size of a few millimeters. In relation to climate change and other environmental events, ferns can also provide insights into adaptation, for example, they survived periods of high CO₂ levels. Only a handful of species have been used to delve into basic developmental processes, such as photomorphogenesis [1], spore germination [2–4], cell polarity [5], cell wall composition [6], or reproduction. These studies focused on the gametophyte

generation, constituted by an autonomously growing organism, which is well-suited for in vitro culture and sample collection [7,8]. Although fern gametophytes possess a very simple structure consisting mostly of a one-cell-thick layer, they display some degree of complexity: apical-basal polarity, dorsoventral asymmetry, rhizoids, meristems in the apical or lateral parts, reproductive organs (male antheridia and female archegonia), and trichomes distributed over the entire surface.

From a metabolic point of view, ferns and lycophytes contain many secondary metabolites, such as flavonoids, alkaloids, phenols, steroids, etc., and exhibit various bioactivities, including antibacterial, antidiabetic, anticancer, antioxidant, etc. [9]. The therapeutic use of both plant groups is changing from its use in the traditional medicine of different peoples to current applications, in which these plants are used to generate nanoparticles [10]. Finally, the use of ferns and lycophytes was recently advocated to address problems caused by biotic and abiotic stresses. Drought is one of the most severe abiotic stresses affecting plant growth and productivity, and ferns and lycophytes could contribute to better understanding and managing it [11]. Other important adaptations of ferns to extreme environments, such as salinity, heavy metals, epiphytes, or a low invasion of their habitats, were summarized by Rathinasabapathi [12]. Likewise, Dhir [13] highlights the high efficiency of many species of aquatic and terrestrial ferns in extracting various organic and inorganic pollutants from the environment. Recently, researchers have become more interested in these plants, which has been made possible by the advent of high-throughput technologies, such as transcriptomics, proteomics, and metabolomics. In fact, performing molecular analyses in ferns has been elusive, as they exhibit higher chromosome numbers and larger genomes than mosses and seed plants [14], which made it difficult to obtain genomic data. Gene expression, induced by either environmental or developmental conditions, can now be examined in non-model organisms because the required techniques have become more affordable as automation and efficiency have reduced costs.

Some transcriptomic and proteomic datasets have been published for ferns during the last decade. First, physiological and proteome analyses were reported with regard to the mechanism of drought tolerance in the resurrection lycophyte *Selaginella tamariscina* [11]. In 2011, the transcriptome of *Pteridium aquilinum* gametophytes was characterized de novo by pyrosequencing, representing the first complete analysis of the transcriptome of a fern [15]. In the same year, a proteomic analysis of the roots of *Pteris vittata* under arsenic stress was carried out [16]. In *Blechnum spicant*, proteomic profiles of male and female gametophytes were reported, revealing an increase in the amount of defense and stress proteins and a decrease in protein synthesis and photosynthesis when inducing male gametophyte development with antheridiogen pheromones [17]. In 2014, a de novo transcriptome assembly of *Lygodium japonicum* was carried out, and with this information a public database was created: Ljtrans DB [18]. Likewise, proteomic and cytological studies associated with germination and growth of rhizoid tips in the fern *Osmunda cinnamomea* were conducted [4]. In the tree fern *Cyathea delgadii*, a proteomic analysis on stipe explants revealed differentially expressed proteins associated with direct somatic embryogenesis [19]. Overlapping patterns of gene expression in gametophytes and sporophytes of the species *Polypodium amorphum* were analyzed by Sigel and colleagues [20], and in the Himalayan fern *Diplazium maximum*, proteomic analysis revealed multiple adaptive response mechanisms to cope with abiotic stresses [21]. Concerning reproduction, sexual versus apomictic expression profiles were analyzed in *Ceratopteris thalictroides* [22], as well as in the species *Adiantum reniforme* var. *sinense* [23]. In addition, some molecular studies were performed on the fern *Ceratopteris richardii* [5,24]; in one of them, sex determination was found to be accompanied by changes in the transcriptome driving epigenetic reprogramming of the young gametophyte [25]; in another, the *WUSCHEL*-related *homeobox* (*WOX*) gene, which promotes cell division in gametophytes and organ development in sporophytes, was characterized for the first time in ferns [26]; and finally, transcriptional analysis of the young sporophyte showed the conservation of stem cell factors in the root apical meristem [27]. More recently, other studies on ferns were carried out. In 2022, the first complete transcriptome of multiple

organs of the fern *Alsophila spinulosa* was obtained, highlighting genes resistant to light stress [28]; its genome was also assembled and characterized; stem anatomy and lignin biosynthesis were investigated [29]; and transcriptomes of several fern species were compared in order to study the adaptive evolution of leaf and root morphology [30]. With the ferns *Dryopteris affinis* ssp. *affinis* [31–33] and *Dryopteris oreades* [33,34], both transcriptomic and proteomic analyses were performed by RNA-sequencing and shotgun proteomics using tandem mass spectrometry.

The current work expands our knowledge of proteomic data in ferns, which are far less explored than in seed plants. We present a continuation of previous work [21] on *D. affinis* ssp. *affinis* (referred to as *D. affinis* hereafter) and its relative *D. oreades*. We have chosen these species as study models because they represent the two types of reproduction present in fern gametophytes: sexual in *D. oreades* and apomictic in *D. affinis*. Proteins of heart-shaped gametophytes were extracted and identified using a species-specific transcriptome database established in a previous project [31–33]. The functional annotation was inferred by blasting identified full-length protein sequences. We report the categorization of proteins that are shared by both sexual and apomictic gametophytes. Specifically, our analysis reveals new proteomic information involved in the metabolism of carbohydrates and lipids, the biosynthesis of amino acids, the metabolism of nucleotides and energy, as well as of secondary compounds, such as flavonoids, terpenoids, lignans, etc., which are important in the plant's defense against stress. In addition, proteins related to transcription, translation, as well as protein folding, sorting, transport, and degradation are reported.

2. Results

A set of 218 proteins shared by the gametophytes of the apomictic fern *D. affinis* (DA) and its sexual relative *D. oreades* (DO) were analyzed using the software programs STRING version 11.5 and CYTOSCAPE version 3.9.1. Proteomic data are available online: <https://www.frontiersin.org/articles/10.3389/fpls.2021.718932/full#supplementary-material> (accessed on 23 June 2023). Therefore, the present work completes previous studies in which 206 and 166 proteins, upregulated in the apomictic and sexual gametophytes, respectively, were analyzed by means of bioinformatic tools, as well as 145 proteins of the remaining 417 that were present in equal amounts in both apomictic and sexual gametophytes. In the present work, the biological functions of the list of 218 proteins were analyzed by using informatic support such as Gene Ontology (GO) and the Kyoto Encyclopedia of Genes and Genomes (KEGG) classifications provided by the STRING platform (Figures 1 and 2). Based on GO classification, most of the identified proteins are involved in known biological functions. In summary, the percentage of proteins associated with the following biological functions are as follows: metabolism of carbohydrates (11.5%), lipids (1.8%), nucleotides (2.2%), biosynthesis of amino acids (6.8%), energy (15.1%), genetic information processing (26.6%), protein folding, sorting and degradation (26.6%), nitrogen and sulfur metabolism (1.8%), and secondary metabolism, including proteins coping with abiotic stress (15.1%).

Some relevant proteins found that will be discussed below are: GLYCINE-RICH RNA-BINDING PROTEIN 3 (RBG3), classified in the group transcription and translation, which functions in RNA processing during stress; FERREDOXIN-NITRITE REDUCTASE 1 (NIR1), grouped in sulfur and nitrogen metabolism, the main activities of which are the reduction of nitrite to ammonium and the improvement of plant assimilation of NO₂; the protein ENOYL-[ACYL-CARRIER-PROTEIN] REDUCTASE (MOD1), classified in the group metabolism of lipids, involved in fatty acid synthesis and plant morphology; CHALCONE-FLAVANONE ISOMERASE 1 (CHI1), related to the group metabolism of secondary compounds and involved in the flavonoid synthesis; and PROTEIN TRANSLOCASE SUBUNIT SECA1 (SECA1), classified in the group transport, active in protein transfer across thylakoid membrane and plant acclimation. In addition, we found the following proteins in the gametophytes: THYLAKOID LUMENAL 16.5 kDa, grouped in the metabolism of energy and involved in photosynthesis; PHOTOSYNTHETIC NDH SUBUNIT OF LUMENAL LOCATION 5 IC (PNLS5), a protein also classified in the group metabolism of energy

that binds to the promoter of the gene *FLOWERING LOCUS D* and represses its expression; ELONGATION FACTOR 2 (LOS1), related to the group transcription and translation and involved in the response to cold; and the protein LEUCINE AMINOPEPTIDASE 1 (LAP1), a chaperone protecting proteins from heat-induced damage.

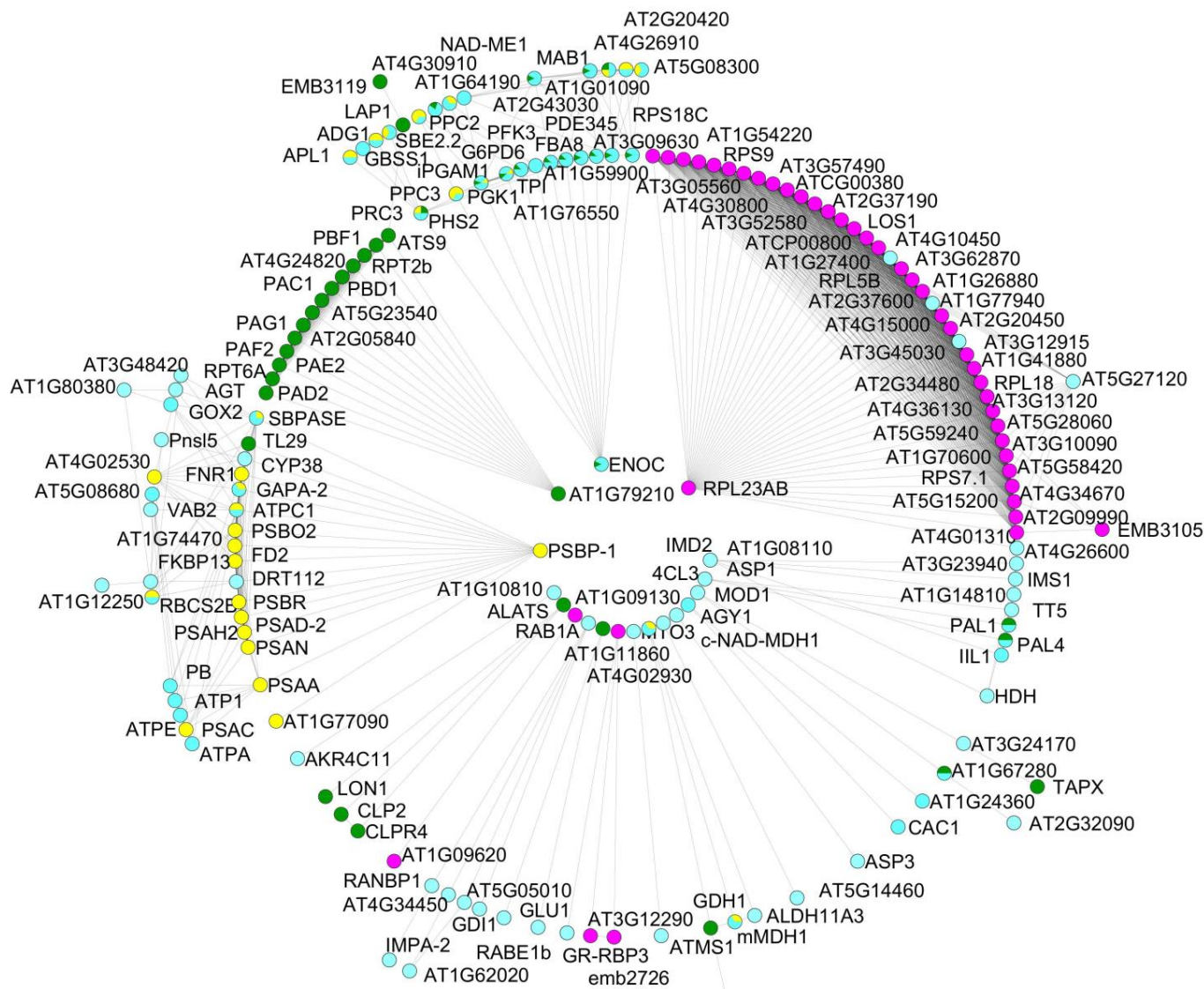


Figure 1. GO enrichment terms of the proteomes shared by gametophytes of *D. affinis* and *D. oreades* according to the category biological function; analyzed by STRING and CYTOSCAPE. Turquoise indicates metabolism of carbohydrates, yellow metabolism of energy, pink transcription and translation, and green protein degradation.

KEGG classification also revealed that common proteins are mostly associated with the biosynthesis of secondary metabolites, the ribosome, the biosynthesis of amino acids, and protein degradation. These processes include the building of cellular organelles, such as ribosomes or proteasomes (Table 1). Related to ribosomes, there were several protein classes, such as nucleic acid-binding proteins, ribosomal proteins, translation elongation factors, etc. On the other hand, proteasomes mediate the degradation of proteins, and we found proteins of the 20S particle, the proteolytic core, but also regulatory factors.

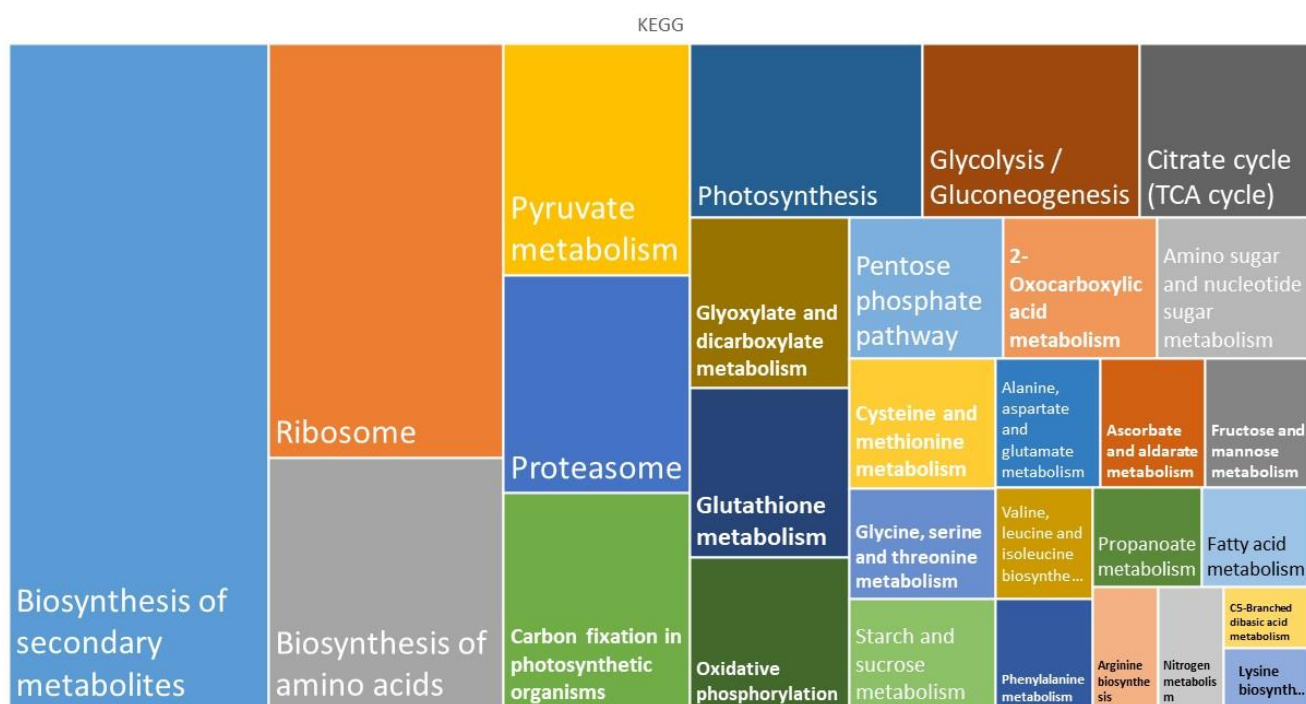


Figure 2. KEGG enrichment terms of the proteomes shared by gametophytes of *D. affinis* and *D. oreades*; analyzed using the STRING platform.

Protein domains that are abundant in the gametophytes of both ferns were the pyruvate dehydrogenase E1 component and the histidine and lysine active sites of the phosphoenolpyruvate carboxylase, which is involved in carbohydrate metabolism. Regarding the biosynthesis of amino acids, the most abundant domains were aspartate aminotransferase and pyridoxal phosphate-dependent transferase. Among proteins involved in the metabolism of energy, the HAS barrel domain and the F1 complex of the alpha and beta subunits of ATP synthase were abundant. Related to the metabolism of secondary compounds, aromatic amino acid lyase, phenylalanine ammonia-lyase, and the N-terminus of histidase were enriched. Finally, the frequently found domains in proteins involved in transcription and translation were the GTP-binding domain and domain 2 of elongation factor Tu, as well as conserved sites of the ribosomal proteins S10 and S4.

The interactome of the proteins common to *D. affinis* and *D. oreades* represented a network composed of 218 nodes and 1792 interactions (p -value < 0.0001). The proteins with the highest number of interactions among the identified proteins are shown in Table 2: LARGE RIBOSOMAL SUBUNIT PROTEIN UL4Z (RPL4A), SMALL RIBOSOMAL SUBUNIT PROTEIN US11X (RPS14C), and SMALL RIBOSOMAL SUBUNIT PROTEIN US17Y (RPS11B) each have 44 interactions.

Table 1. Proteins involved in ribogenesis and protein degradation found in the gametophyte of the ferns *D. affinis* and *D. oreades*.

| Category | Accession Number | UniProtKB/ Swiss-Prot | Gene Name | Protein Name | MW (kDa) | % Coverage | Exclusive Unique Peptides | Total Spectrum | E-Value |
|-------------|-------------------|--------------------------|----------------|---|-------------|---------------|---------------------------------|-------------------|-------------------------|
| Ribogenesis | 1-12177_3_ORF5 | P56799 | <i>RPS4</i> | SMALL RIBOSOMAL SUBUNIT PROTEIN US4C | 25.6 | 0 | 0 | 3 | 7.63×10^{-70} |
| Ribogenesis | 16646-605_4_ORF2 | Q9SX68 | <i>RPL18</i> | LARGE RIBOSOMAL SUBUNIT PROTEIN UL18C | 20.9 | 7 | 1 | 3 | 7.35×10^{-57} |
| Ribogenesis | 24557-506_3_ORF2 | Q9SKX4 | <i>RPL3A</i> | LARGE RIBOSOMAL SUBUNIT PROTEIN UL3C | 29.3 | 14 | 2 | 9 | 5.37×10^{-121} |
| Ribogenesis | 139931-207_5_ORF1 | O04603 | <i>RPL5</i> | LARGE RIBOSOMAL SUBUNIT PROTEIN UL5C | 32.4 | 8 | 2 | 14 | 2.41×10^{-92} |
| Ribogenesis | 26987-486_4_ORF2 | Q9M3C3 | <i>RPL23AB</i> | LARGE RIBOSOMAL SUBUNIT PROTEIN UL23Y | 20.2 | 31 | 1 | 39 | 3.98×10^{-60} |
| Ribogenesis | 6809-878_4_ORF2 | P49227 | <i>RPL5B</i> | LARGE RIBOSOMAL SUBUNIT PROTEIN UL18Y | 34.7 | 13 | 4 | 12 | 1.09×10^{-53} |
| Ribogenesis | 87113-269_4_ORF1 | Q9M9W1 | <i>RPL22B</i> | LARGE RIBOSOMAL SUBUNIT PROTEIN EL22Z | 16.1 | 14 | 1 | 3 | 1.35×10^{-52} |
| Ribogenesis | 21899-533_1_ORF2 | P51419 | <i>RPL27C</i> | LARGE RIBOSOMAL SUBUNIT PROTEIN EL27X | 18.2 | 19 | 3 | 22 | 7.19×10^{-65} |
| Ribogenesis | 24282-509_2_ORF1 | P50883 | <i>RPL12A</i> | LARGE RIBOSOMAL SUBUNIT PROTEIN UL11Z | 19.1 | 13 | 0 | 6 | 1.24×10^{-104} |
| Ribogenesis | 36225-421_1_ORF2 | Q9SIM4 | <i>RPL14A</i> | LARGE RIBOSOMAL SUBUNIT PROTEIN EL14Z | 17.9 | 19 | 2 | 11 | 2.62×10^{-68} |
| Ribogenesis | 10983-723_3_ORF2 | P51418 | <i>RPL18AB</i> | LARGE RIBOSOMAL SUBUNIT PROTEIN EL20Y | 22.9 | 10 | 1 | 9 | 1.99×10^{-119} |
| Ribogenesis | 34727-430_6_ORF2 | P49637 | <i>RPL27AC</i> | LARGE RIBOSOMAL SUBUNIT PROTEIN UL15X | 16.3 | 7 | 1 | 4 | 8.73×10^{-78} |
| Ribogenesis | 73912-293_6_ORF2 | Q42064 | <i>RPL8C</i> | LARGE RIBOSOMAL SUBUNIT PROTEIN UL2X | 28.7 | 25 | 4 | 42 | 2.24×10^{-167} |
| Ribogenesis | 37807-413_3_ORF1 | Q93VI3 | <i>RPL17A</i> | LARGE RIBOSOMAL SUBUNIT PROTEIN UL22Z | 23.5 | 4 | 1 | 7 | 5.22×10^{-107} |
| Ribogenesis | 176389-160_3_ORF2 | Q42351 | <i>RPL34A</i> | LARGE RIBOSOMAL SUBUNIT PROTEIN EL34Z | 18.2 | 12 | 1 | 15 | 1.23×10^{-65} |
| Ribogenesis | 8788-797_5_ORF2 | Q9FZH0 | <i>RPL35AB</i> | LARGE RIBOSOMAL SUBUNIT PROTEIN EL33Z | 13.6 | 18 | 0 | 17 | 6.54×10^{-60} |
| Ribogenesis | 27503-481_2_ORF2 | O80929 | <i>RPL36A</i> | LARGE RIBOSOMAL SUBUNIT PROTEIN EL36Z | 13 | 16 | 1 | 28 | 8.82×10^{-52} |
| Ribogenesis | 75664-290_4_ORF2 | Q9SF40 | <i>RPL4A</i> | LARGE RIBOSOMAL SUBUNIT PROTEIN UL4Z | 46.3 | 12 | 3 | 20 | 0 |
| Ribogenesis | 45247-378_5_ORF2 | Q9SZX9 | <i>RPL9D</i> | LARGE RIBOSOMAL SUBUNIT PROTEIN UL6X | 25.1 | 7 | 1 | 11 | 1.63×10^{-105} |
| Ribogenesis | 86488-270_3_ORF2 | Q9LZH9 | <i>RPL7AB</i> | LARGE RIBOSOMAL SUBUNIT PROTEIN EL8Y | 32.5 | 26 | 8 | 33 | 7.63×10^{-154} |
| Ribogenesis | 163051-176_2_ORF2 | Q8VZ19 | <i>RPL30B</i> | LARGE RIBOSOMAL SUBUNIT PROTEIN EL30Y | 16.7 | 13 | 2 | 9 | 1.91×10^{-61} |
| Ribogenesis | 69050-304_1_ORF1 | P49200 | <i>RPS20A</i> | SMALL RIBOSOMAL SUBUNIT PROTEIN US10Z | 21.1 | 12 | 2 | 14 | 3.32×10^{-72} |
| Ribogenesis | 5816-941_6_ORF2 | P42036 | <i>RPS14C</i> | SMALL RIBOSOMAL SUBUNIT PROTEIN US11X | 18.7 | 22 | 3 | 7 | 2.52×10^{-87} |
| Ribogenesis | 39126-407_1_ORF2 | Q8LC83 | <i>RPS24B</i> | SMALL RIBOSOMAL SUBUNIT PROTEIN ES24Y | 20.7 | 7 | 1 | 2 | 8.38×10^{-74} |
| Ribogenesis | 108940-238_6_ORF2 | Q42262 | <i>RPS3AB</i> | SMALL RIBOSOMAL SUBUNIT PROTEIN ES1Y | 32.7 | 22 | 5 | 21 | 8.87×10^{-155} |
| Ribogenesis | 85164-272_6_ORF2 | Q8VYK6 | <i>RPS4D</i> | SMALL RIBOSOMAL SUBUNIT PROTEIN ES4X | 30 | 7 | 2 | 18 | 9.28×10^{-165} |
| Ribogenesis | 45770-376_1_ORF2 | Q9LXG1 | <i>RPS9B</i> | SMALL RIBOSOMAL SUBUNIT PROTEIN US4Z | 24.7 | 4 | 0 | 9 | 1.32×10^{-121} |
| Ribogenesis | 140134-206_2_ORF2 | F4JB06 | <i>MGH6.2</i> | RIBOSOMAL PROTEIN S5/ELONGATION FACTOR G/III/V FAMILY PROTEIN | 16.9 | 7 | 0 | 1 | 2×10^{-50} |
| Ribogenesis | 1627-1498_1_ORF1 | P61841 | <i>RPS7-A</i> | SMALL RIBOSOMAL SUBUNIT PROTEIN US7CZ | 18.8 | 13 | 3 | 11 | 3.24×10^{-77} |
| Ribogenesis | 31704-450_4_ORF1 | Q9FIF3 | <i>ES8Y</i> | RIBOSOMAL PROTEIN ES8Y | 16.8 | 28 | 1 | 19 | 1.93×10^{-73} |
| Ribogenesis | 11320-714_2_ORF2 | Q9XJ27 | <i>RPS9</i> | SMALL RIBOSOMAL SUBUNIT PROTEIN US9C | 25.9 | 3 | 1 | 3 | 1.03×10^{-76} |
| Ribogenesis | 21394-539_3_ORF2 | P42791 | <i>RPL18B</i> | LARGE RIBOSOMAL SUBUNIT PROTEIN EL18Y | 23.4 | 25 | 3 | 21 | 1.03×10^{-105} |
| Ribogenesis | 40578-399_1_ORF2 | P56798 | <i>RPS3</i> | SMALL RIBOSOMAL SUBUNIT PROTEIN US3C | 25.3 | 6 | 1 | 6 | 6.73×10^{-82} |
| Ribogenesis | 10791-728_3_ORF2 | O65569 | <i>RPS11B</i> | SMALL RIBOSOMAL SUBUNIT PROTEIN US17Y | 20.5 | 12 | 2 | 36 | 5.17×10^{-84} |
| Ribogenesis | 66444-310_2_ORF2 | Q1PEP5 | <i>NUCL2</i> | NUCLEOLIN 2 | 61.5 | 12 | 6 | 11 | 6.83×10^{-49} |

Table 1. Cont.

| Category | Accession Number | UniProtKB/ Swiss-Prot | Gene Name | Protein Name | MW (kDa) | % Coverage | Exclusive Unique Peptides | Total Spectrum | E-Value |
|-------------|------------------|--------------------------|---------------|--|-------------|---------------|---------------------------------|-------------------|-------------------------|
| Ribogenesis | 260531-93_3_ORF2 | O04658 | <i>NOP5-1</i> | PROBABLE NUCLEOLAR PROTEIN 5-1 | 62.5 | 11 | 5 | 10 | 0 |
| Proteasome | 93086-259_4_ORF1 | Q9LT08 | <i>RPN11</i> | 26S PROTEASOME NON-ATPASE REGULATORY SUBUNIT 14 HOMOLOG | 34.9 | 3 | 1 | 5 | 0 |
| Proteasome | 78122-285_4_ORF2 | Q93Y35 | <i>RPN7</i> | 26S PROTEASOME NON-ATPASE REGULATORY SUBUNIT 6 HOMOLOG | 44.8 | 4 | 1 | 9 | 0 |
| Proteasome | 353924-42_4_ORF1 | O23712 | <i>PAF2</i> | PROTEASOME SUBUNIT ALPHA TYPE-1-B | 13.9 | 8 | 1 | 2 | 2.8×10^{-136} |
| Proteasome | 7073-864_3_ORF1 | O23708 | <i>PAB1</i> | PROTEASOME SUBUNIT ALPHA TYPE-2-A | 26.4 | 9 | 2 | 10 | 4.87×10^{-158} |
| Proteasome | 326729-54_1_ORF2 | O81148 | <i>PAC1</i> | PROTEASOME SUBUNIT ALPHA TYPE-4-A | 30.6 | 13 | 3 | 9 | 3.69×10^{-154} |
| Proteasome | 68626-305_4_ORF2 | Q42134 | <i>PAE2</i> | PROTEASOME SUBUNIT ALPHA TYPE-5-B | 28.7 | 28 | 3 | 13 | 4.68×10^{-158} |
| Proteasome | 23928-513_3_ORF1 | O81147 | <i>PAA2</i> | PROTEASOME SUBUNIT ALPHA TYPE-6-B | 30.8 | 7 | 3 | 12 | 9.67×10^{-153} |
| Proteasome | 340935-47_4_ORF1 | O24616 | <i>PAD2</i> | PROTEASOME SUBUNIT ALPHA TYPE-7-B | 27.4 | 18 | 4 | 11 | 3.86×10^{-148} |
| Proteasome | 14462-637_1_ORF2 | O23714 | <i>PBD1</i> | PROTEASOME SUBUNIT BETA TYPE-2-A | 24.3 | 4 | 1 | 7 | 1.43×10^{-103} |

Table 2. Biological functions and number of interactions exhibited by proteins common to apomictic *D. affinis* and sexual *D. oreades*.

| Biological Function | Protein | N° of Interactions |
|-----------------------------|---------------------------------------|--------------------|
| Metabolism of carbohydrates | PHOSPHOGLYCERATE KINASE 1 | 11 |
| | 3-ISOPROPYLMALATE DEHYDROGENASE | 5 |
| Biosynthesis of amino acids | DIHYDROXY-ACID DEHYDRATASE | 5 |
| | ASPARTATE-SEMIALDEHYDE DEHYDROGENASE | 5 |
| Metabolism of energy | ATP SYNTHASE GAMMA CHAIN 1 | 18 |
| Secondary metabolism | 4-COUMARATE-COA LIGASE 3 | 3 |
| | LARGE RIBOSOMAL SUBUNIT PROTEIN UL4Z | 44 |
| Transcription & Translation | SMALL RIBOSOMAL SUBUNIT PROTEIN US11X | 44 |
| | SMALL RIBOSOMAL SUBUNIT PROTEIN US17Y | 44 |
| Transport | PROTEIN TRANSLOCASE SUBUNIT SECA1 | 2 |
| | COATOMER SUBUNIT GAMMA | 2 |

The strength of the interactions can be weak or strong (Table S1), using a scale from 0 to 1 where a weak interaction will have a score close to 0 and a strong one a score close to 1. Taking only interactions with a score equal to or greater than 0.99 for each group of proteins studied into account, proteins involved in transcription and translation are those with the highest number of interactions (554), followed by proteins involved in energy (29), carbohydrate metabolism (16), biosynthesis of amino acids (5), and transport (3). According to the STRING software v.11, the evidence of interactions between proteins can be of various types: (a) Experiments: these refer to proteins that have been shown to have chemical, physical, or genetic interaction in laboratory experiments. (b) Databases: this describes interactions of proteins found in the same databases. (c) Text mining: the proteins are mentioned in the same PubMed abstract or the same article of an internal selection of the STRING software v.11. (d) Co-expression: this indicates that the expression patterns of the two proteins are similar. (e) Neighborhood: the genes encoding the proteins are close to each other in the genome. (f) Gene fusion: this indicates that at least in one organism the orthologous genes encoding the two proteins are fused into a single gene. (g) Co-occurrence: this refers to proteins that have a similar phylogenetic distribution. The interactome presented here uses the species *Arabidopsis thaliana* because all the proteins discussed later were found to be homologs of proteins in this species. Therefore, the protein–protein interactions are those expected to be found in *A. thaliana*. On the other hand, STRING collects information from several sources and proposes protein–protein interactions according to the deposited data. We chose to explore all the types of protein–protein interactions published in the STRING platform for our selected proteins.

Next, we consider some of these types of interaction between proteins (Figure 3: text mining, experiments, co-expression, and databases). Specifically, we focused on the group metabolism of carbohydrates (Figure 3a), metabolism of energy (Figure 3b), ribogenesis (Figure 3c), and protein degradation (Figure 3d). Paying attention only to the two main types of evidence for each of these groups, their relationships were analyzed (Figure 4). Evidence from databases and text mining were the most relevant for the metabolism of carbohydrates (Figure 4a), biosynthesis of amino acids (Figure 4b), the metabolism of secondary compounds, and transport, as well as text mining and co-expression data for the metabolism of energy (Figure 4c), and experiments and co-expression data for transcription and translation (Figure 4d). The significance of associations between variables were as follows: in the metabolism of carbohydrates and in the transcription and translation, highly significant in both (p -value < 0.001); in the biosynthesis of amino acids, not significant (p -value > 0.05); and in the metabolism of energy, marginally significant (p -value slightly greater than 0.05).

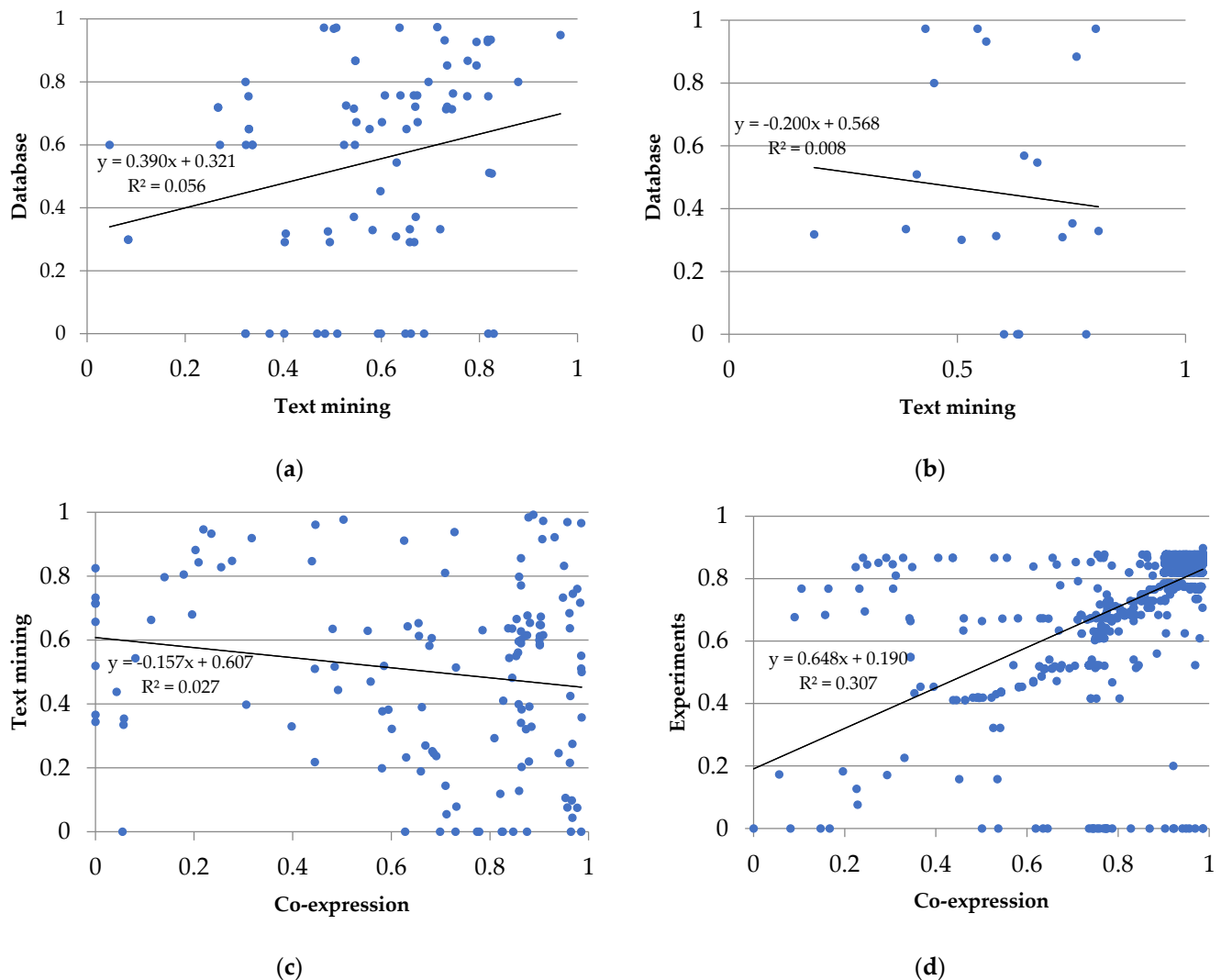


Figure 4. Plots of the two main types of evidence for interactions in the groups of proteins shared by the gametophytes of *D. affinis* and *D. oreades*: (a) metabolism of carbohydrates, (b) biosynthesis of amino acids, (c) metabolism of energy, and (d) transcription and translation. Each spot represents the intersection of the type of evidence for interactions between two proteins. The linear regression and the coefficient of correlation are provided for each pair of evidence for the interaction.

3. Discussion

Molecular research conducted in non-model species, such as ferns and lycophytes, is still scarce. These plant groups are the last major lineage of land plants without a reference genome. Their higher chromosome numbers and larger genomes compared to those of mosses and seed plants have contributed to the paucity of reports dealing with genomic or proteomic analyses. Much more effort is needed to broaden the number of species analyzed to complete our knowledge of plant development. Thus, the current work provides novel information on the proteome shared by gametophytes of the apomictic fern *D. affinis* and its sexual relative *D. oreades*, and extends and completes previous studies in these species [31–34].

Next, we discuss the biological functions and interactions between the set of proteins obtained, which are grouped into three major categories: metabolism, genetic information processing, and response to abiotic stress (Table 3).

Table 3. Selected proteins found in gametophytes of both apomictic *D. affinis* and sexual *D. oreades*.

| Category | Accession Number | UniProtKB/ Swiss-Prot | Gene Name | Protein Name | MW (kDa) | % Coverage | Exclusive Unique Peptides | Total Spectra | E-Value |
|---------------|-------------------|--------------------------|------------------|--|-------------|---------------|---------------------------------|------------------|-------------------------|
| Carbohydrates | 58787-330_2_ORF2 | Q94AA4 | <i>PFK3</i> | ATP-DEPENDENT 6-PHOSPHOFRUCTOKINASE 3 | 64.5 | 2 | 1 | 1 | 0 |
| Carbohydrates | 135690-210_1_ORF2 | Q9ZU52 | <i>FBA3</i> | FRUCTOSE-BISPHOSPHATE ALDOLASE 3 | 42.7 | 32 | 7 | 38 | 0 |
| Carbohydrates | 38153-411_5_ORF2 | Q38799 | <i>PDH2</i> | PYRUVATE DEHYDROGENASE E1 COMPONENT SUBUNIT BETA-1 | 40.3 | 14 | 4 | 6 | 0 |
| Carbohydrates | 83096-276_3_ORF2 | Q5GM68 | <i>PPC2</i> | PHOSPHOENOLPYRUVATE CARBOXYLASE 2 | 112.8 | 6 | 5 | 5 | 0 |
| Carbohydrates | 54280-344_1_ORF1 | Q84VW9 | <i>PPC3</i> | PHOSPHOENOLPYRUVATE CARBOXYLASE 3 | 111.8 | 1 | 0 | 1 | 0 |
| Carbohydrates | 113756-233_2_ORF1 | Q9SIU0 | <i>NAD-ME1</i> | NAD-DEPENDENT MALIC ENZYME 1 | 71.4 | 3 | 2 | 3 | 0 |
| Carbohydrates | 102811-246_6_ORF2 | O04499 | <i>PGM1</i> | 2,3-BIPHOSPHOGLYCERATE-INDEPENDENT PHOSPHOGLYCERATE MUTASE 1 | 63.2 | 4 | 1 | 2 | 0 |
| Carbohydrates | 64100-316_1_ORF1 | O82662 | <i>AT2G20420</i> | SUCCINATE-COA LIGASE [ADP-FORMING] SUBUNIT BETA | 50 | 9 | 0 | 4 | 0 |
| Carbohydrates | 8279-816_3_ORF2 | P68209 | <i>AT5G08300</i> | SUCCINATE-COA LIGASE [ADP-FORMING] SUBUNIT ALPHA-1 | 34.6 | 9 | 2 | 3 | 0 |
| Carbohydrates | 222487-119_2_ORF2 | P93819 | <i>MDH1</i> | MALATE DEHYDROGENASE 1 | 38.4 | 20 | 2 | 16 | 0 |
| Carbohydrates | 156827-185_4_ORF1 | Q9SH69 | <i>PGD1</i> | 6-PHOSPHOGLUCONATE DEHYDROGENASE, DECARBOXYLATING 1 | 58.8 | 16 | 2 | 9 | 1.37×10^{-112} |
| Carbohydrates | 12493-682_6_ORF2 | Q9FJ15 | <i>G6PD6</i> | GLUCOSE-6-PHOSPHATE 1-DEHYDROGENASE 6 | 65.1 | 6 | 3 | 3 | 0 |
| Carbohydrates | 20760-547_4_ORF1 | Q9LD57 | <i>PGK1</i> | PHOSPHOGLYCERATE KINASE 1 | 19.5 | 14 | 0 | 3 | 5.63×10^{-43} |
| Carbohydrates | 69882-302_6_ORF2 | Q9LZS3 | <i>SBE2.2</i> | 1,4-ALPHA-GLUCAN-BRANCHING ENZYME 2-2 | 98.6 | 5 | 4 | 6 | 0 |
| Carbohydrates | 96049-255_6_ORF1 | Q9MAQ0 | <i>GBSS1</i> | GRANULE BOUND STARCH SYNTHASE 1 | 70.16 | 1 | 1 | 1 | 0 |
| Lipids | 20213-554_2_ORF1 | Q9SLA8 | <i>MOD1</i> | ENOYL-[ACYL-CARRIER-PROTEIN] REDUCTASE [NADH] | 41.8 | 7 | 1 | 6 | 4.48×10^{-180} |
| Lipids | 387953-27_4_ORF1 | Q9SGY2 | <i>ACLA-1</i> | ATP-CITRATE SYNTHASE ALPHA CHAIN PROTEIN 1 | 46.8 | 10 | 2 | 4 | 0 |
| Lipids | 211149-128_1_ORF1 | Q9LXS6 | <i>CSY2</i> | CITRATE SYNTHASE 2 | 57.9 | 2 | 0 | 1 | 0 |
| Amino acids | 47558-369_4_ORF2 | P46643 | <i>ASP1</i> | ASPARTATE AMINOTRANSFERASE | 51.5 | 5 | 0 | 5 | 0 |
| Amino acids | 72506-296_4_ORF1 | Q94AR8 | <i>IIL1</i> | 3-ISOPROPYLMALATE DEHYDRATASE LARGE SUBUNIT | 57.6 | 6 | 3 | 4 | 0 |
| Amino acids | 125905-219_3_ORF2 | Q9ZNZ7 | <i>GLU1</i> | FERREDOXIN-DEPENDENT GLUTAMATE SYNTHASE 1 | 181.3 | 6 | 5 | 13 | 0 |
| Amino acids | 14065-645_3_ORF2 | Q9C5U8 | <i>HISN8</i> | HISTIDINOL DEHYDROGENASE | 55.2 | 1 | 2 | 1 | 0 |
| Amino acids | 294436-71_4_ORF2 | Q9LUT2 | <i>METK4</i> | S-ADENOSYLMETHIONINE SYNTHASE 4 | 42.7 | 5 | 0 | 2 | 0 |
| Nucleotides | 2121-1366_3_ORF2 | Q9SF85 | <i>ADK1</i> | ADENOSINE KINASE 1 | 39.2 | 14 | 3 | 4 | 0 |
| Nucleotides | 59309-329_5_ORF1 | Q96529 | <i>PURA</i> | ADENYLOSUCCINATE SYNTHETASE | 57.9 | 2 | 1 | 1 | 0 |
| Nucleotides | 152024-193_3_ORF2 | Q9S726 | <i>RPI3</i> | PROBABLE RIBOSE-5-PHOSPHATE ISOMERASE 3 | 36.1 | 2 | 0 | 2 | 5.33×10^{-120} |
| Nucleotides | 27769-479_3_ORF1 | P55228 | <i>ADG1</i> | GLUCOSE-1-PHOSPHATE ADENYLYLTRANSFERASE SMALL SUBUNIT | 12.5 | 7 | 0 | 1 | 4.43×10^{-63} |
| Nucleotides | 181563-155_3_ORF2 | P55229 | <i>ADG2</i> | GLUCOSE-1-PHOSPHATE ADENYLYLTRANSFERASE LARGE SUBUNIT 1 | 57.4 | 6 | 2 | 4 | 0 |
| Energy | 154679-189_1_ORF2 | Q9S841 | <i>PSBO2</i> | OXYGEN-EVOLVING ENHANCER PROTEIN 1-2 | 35.3 | 35 | 7 | 24 | 6.62×10^{-141} |
| Energy | 218625-122_1_ORF2 | O22773 | <i>AT4G02530</i> | THYLAKOID LUMENAL 16.5 kDa PROTEIN | 24.7 | 5 | 1 | 1 | 8.55×10^{-47} |

Table 3. Cont.

| Category | Accession Number | UniProtKB/ Swiss-Prot | Gene Name | Protein Name | MW (kDa) | % Coverage | Exclusive Unique Peptides | Total Spectra | E-Value |
|---------------------|-------------------|--------------------------|------------------|---|-------------|---------------|---------------------------------|------------------|-------------------------|
| Energy | 6036-926_2_ORF1 | Q9ASS6 | <i>PNSL5</i> | PHOTOSYNTHETIC NDH SUBUNIT OF LUMENAL LOCATION 5 | 32.2 | 15 | 4 | 10 | 2.45×10^{-93} |
| Energy | 250817-99_2_ORF2 | Q94K71 | <i>CBBY</i> | CBBY-LIKE PROTEIN | 34.9 | 7 | 2 | 3 | 6.24×10^{-131} |
| Energy | 235330-110_2_ORF1 | Q944I4 | <i>GLYK</i> | D-GLYCERATE 3-KINASE | 43.9 | 3 | 0 | 1 | 2.82×10^{-153} |
| Energy | 297118-70_2_ORF2 | Q56YA5 | <i>AGT1</i> | SERINE-GLYOXYLATE AMINOTRANSFERASE | 47.8 | 2 | 0 | 2 | 0 |
| S&N metabolism | 33137-439_6_ORF2 | O48917 | <i>SQD1</i> | UDP-SULFOQUINOVOSE SYNTHASE | 54.9 | 10 | 3 | 4 | 0 |
| S&N metabolism | 227095-115_1_ORF2 | Q84W65 | <i>SUFE1</i> | SUFE-LIKE PROTEIN 1 | 40.7 | 2 | 1 | 1 | 3.22×10^{-106} |
| S&N metabolism | 311596-62_2_ORF2 | Q9ZST4 | <i>GLB1</i> | NITROGEN REGULATORY PROTEIN P-II HOMOLOG | 23.4 | 15 | 1 | 1 | 3.28×10^{-62} |
| S&N metabolism | 318906-58_1_ORF1 | Q39161 | <i>NIR1</i> | FERREDOXIN-NITRITE REDUCTASE | 69.6 | 7 | 4 | 8 | 0 |
| Secondary compounds | 156331-186_3_ORF2 | P41088 | <i>CHI1</i> | CHALCONE-FLAVANONE ISOMERASE 1 | 26.2 | 6 | 0 | 2 | 6.89×10^{-56} |
| Secondary compounds | 230420-113_2_ORF2 | P34802 | <i>GGPPS1</i> | HETERODIMERIC GERANYLGERANYL PYROPHOSPHATE SYNTHASE LARGE SUBUNIT 1 | 41 | 5 | 1 | 1 | 1.48×10^{-147} |
| Secondary compounds | 85783-271_1_ORF2 | Q9T030 | <i>PCBER1</i> | PHENYLCOUMARAN BENZYLIC ETHER REDUCTASE 1 | 34.9 | 33 | 9 | 23 | 4.03×10^{-115} |
| Secondary compounds | 156554-185_2_ORF1 | Q9S777 | <i>4CL3</i> | 4-COUMARATE-COA LIGASE 3 | 51.9 | 2 | 1 | 2 | 0 |
| Secondary compounds | 223603-118_1_ORF1 | P05466 | <i>AT2G45300</i> | 3-PHOSPHOSHIMATE 1-CARBOXYVINYLTRANSFERASE | 44.3 | 2 | 1 | 1 | 0 |
| Oxido-reduction | 133847-212_2_ORF2 | Q9SID3 | <i>AT2G31350</i> | HYDROXYACYLGLUTATHIONE HYDROLASE 2 | 33.1 | 6 | 1 | 1 | 6.51×10^{-131} |
| Oxido-reduction | 34437-432_2_ORF1 | Q9M2W2 | <i>GSTL2</i> | GLUTATHIONE S-TRANSFERASE L2 | 16.1 | 15 | 2 | 5 | 3.24×10^{-29} |
| Oxido-reduction | 115571-230_4_ORF1 | Q9LZ06 | <i>GSTL3</i> | GLUTATHIONE S-TRANSFERASE L3 | 35.3 | 1 | 2 | 1 | 6.13×10^{-75} |
| Transcription | 181200-155_2_ORF2 | Q96300 | <i>GRF7</i> | 14-3-3-LIKE PROTEIN GF14 NU | 32.8 | 12 | 1 | 9 | 1.11×10^{-161} |
| Transcription | 287872-75_1_ORF1 | Q9C5W6 | <i>GRF12</i> | 14-3-3-LIKE PROTEIN GF14 IOTA | 32.8 | 12 | 1 | 9 | 3.83×10^{-151} |
| Translation | 209284-130_2_ORF2 | Q9FNR1 | <i>RBG3</i> | GLYCINE-RICH RNA-BINDING PROTEIN 3 | 19.8 | 15 | 2 | 4 | 1.45×10^{-31} |
| Translation | 293356-72_1_ORF1 | Q9LR72 | <i>PCMP-E3</i> | PUTATIVE PENTATRICOPEPTIDE REPEAT-CONTAINING PROTEIN AT1G03510 (POLIPASA) | 26.1 | 5 | 1 | 1 | 0.4 |
| Translation | 26795-487_6_ORF2 | Q0WW84 | <i>RBP47B</i> | POLYADENYLATE-BINDING PROTEIN RBP47B | 45.9 | 2 | 0 | 1 | 3.27×10^{-136} |
| Translation | 174433-162_1_ORF1 | Q9ASR1 | <i>LOS1</i> | ELONGATION FACTOR 2 | 73.8 | 9 | 1 | 12 | 0 |
| Folding | 26640-489_1_ORF2 | Q9M1C2 | <i>CPN10-1</i> | 10 kDa CHAPERONIN 1 | 19.4 | 15 | 2 | 6 | 9.48×10^{-39} |
| Folding | 189606-147_1_ORF2 | Q9SR70 | <i>FKBP16-4</i> | PEPTIDYL-PROLYL CIS-TRANS ISOMERASE FKBP16-4 | 26.4 | 13 | 3 | 6 | 1.35×10^{-89} |
| Folding | 2524-1285_6_ORF2 | Q9SKQ0 | <i>CYP19-2</i> | PEPTIDYL-PROLYL CIS-TRANS ISOMERASE CYP19-2 | 21.6 | 27 | 5 | 24 | 2.24×10^{-90} |
| Sorting | 19573-562_5_ORF2 | Q9SY10 | <i>SECA1</i> | PROTEIN TRANSLOCASE SUBUNIT SECA1 | 115.7 | 2 | 1 | 2 | 0 |
| Sorting | 146969-201_2_ORF1 | F4JL11 | <i>IMPA2</i> | IMPORTIN SUBUNIT ALPHA-2 | 59.1 | 5 | 0 | 2 | 6×10^{-61} |
| Sorting | 151836-193_1_ORF2 | P40941 | <i>AAC2</i> | ADP, ATP CARRIER PROTEIN 2 | 42.3 | 7 | 1 | 5 | 0 |
| Sorting | 161087-178_2_ORF2 | Q8H0U5 | <i>TIC62</i> | PROTEIN TIC 62 | 73.4 | 6 | 4 | 6 | 5.77×10^{-115} |
| Sorting | 82340-277_1_ORF2 | Q39196 | <i>PIP1.4</i> | PROBABLE AQUAPORIN PIP1-4 | 33 | 6 | 2 | 3 | 3.75×10^{-170} |
| Sorting | 272341-85_2_ORF2 | Q94A40 | <i>AT1G62020</i> | COATOMER SUBUNIT ALPHA-1 | 137 | 1 | 0 | 1 | 0 |

Table 3. Cont.

| Category | Accession Number | UniProtKB/ Swiss-Prot | Gene Name | Protein Name | MW (kDa) | % Coverage | Exclusive Unique Peptides | Total Spectra | E-Value |
|-------------|-------------------|--------------------------|-----------|---|-------------|---------------|---------------------------------|------------------|-------------------------|
| Sorting | 29489-466_3_ORF1 | Q0WW26 | AT4G34450 | COATOMER SUBUNIT GAMMA | 103 | 2 | 1 | 1 | 0 |
| Sorting | 43675-385_1_ORF2 | Q67YI9 | EPSIN2 | CLATHRIN INTERACTOR EPSIN 2 | 85.2 | 1 | 1 | 1 | 1.51×10^{-117} |
| Sorting | 68824-304_5_ORF2 | Q9LQ55 | DRP2B | DYNAMIN-2B | 105.3 | 1 | 1 | 1 | 0 |
| Degradation | 141778-205_4_ORF2 | Q8L770 | CLPR3 | ATP-DEPENDENT CLP PROTEASE PROTEOLYTIC SUBUNIT-RELATED PROTEIN 3 | 38.9 | 2 | 1 | 1 | 1.73×10^{-136} |
| Degradation | 172993-163_5_ORF1 | Q9XJ36 | CLPR2 | ATP-DEPENDENT CLP PROTEASE PROTEOLYTIC SUBUNIT-RELATED PROTEIN 2 | 32.7 | 4 | 1 | 1 | 4.49×10^{-126} |
| Degradation | 170504-166_2_ORF2 | P30184 | LAP1 | LEUCINE AMINOPEPTIDASE 1 | 62.5 | 4 | 1 | 4 | 0 |

3.1. Metabolism

Primary and secondary metabolism encompasses a great number of enzymes connecting all the chemical pathways associated with them. Therefore, proteomic analyses usually yield a lot of proteins linked to the biosynthesis or degradation of carbohydrates, lipids, proteins, and nucleotides, as well as others that, albeit being called secondary, are not less important. Additionally, proteins linked to the metabolism of energy mediated by processes such as photosynthesis or photorespiration are commonly reported as well.

Carbohydrates

Within this metabolic group, the process of glycolysis converts glucose into pyruvate, and in the gametophytes under study, we found enzymes, such as ATP-DEPENDENT 6-PHOSPHOFRUCTOKINASE 3 (PFK3), involved in the first reaction, two enzymes participating in glycolysis and gluconeogenesis, FRUCTOSE-BISPHOSPHATE ALDOLASE 3 (FBA3), and others catalyzing the decarboxylation of pyruvate to acetyl-CoA, such as PYRUVATE DEHYDROGENASE E1 COMPONENT SUBUNIT BETA-1 (PDH2). The protein FBA3 reported here and also the protein FBA8 were identified in studies of the fern *C. delgadii* [19]. Linked to pyruvate metabolism, we identified two phosphoenolpyruvate carboxylases (PPC2 and PPC3), which supply oxaloacetate for the tricarboxylic acid cycle, and the protein NAD-DEPENDENT MALIC ENZYME 1 (NAD-ME1), which is involved in regulating the metabolism of sugars and amino acids during the night [35]. Worth mentioning is also 2,3-BIPHOSPHOGLYCERATE-INDEPENDENT PHOSPHOGLYCERATE MUTASE 1 (PGM1), which is important for the functioning of stomatal guard cells and fertility in *A. thaliana* [36]. Gametophytes of *D. affinis* and *D. oreades* produce proteins involved in starch synthesis, including 1,4-ALPHA-GLUCAN-BRANCHING ENZYME 2-2 (SBE2.2) and GRANULE-BOUND STARCH SYNTHASE 1 (GBSS1).

Tricarboxylic acid cycle and pentose phosphate pathway

Likewise, we identified some proteins associated with the citrate/tricarboxylic acid cycle, SUCCINATE-CoA LIGASE [ADP-FORMING] SUBUNIT BETA (AT2G20420) and SUCCINATE-CoA LIGASE [ADP-FORMING] SUBUNIT ALPHA-1 (AT5G08300), which are involved in the only phosphorylation step at the substrate level of this cycle. Another protein is MALATE DEHYDROGENASE 1 (MDH1), which catalyzes a reversible NAD-dependent dehydrogenase reaction involved in central metabolism and redox homeostasis between organelle compartments [37]. This protein was also found in three ferns: *P. vittata*, when studying the response to arsenic stress in the roots with or without arbuscular mycorrhizal symbiosis [16]; in germinating spores of *O. cinnamomea* [4]; and in sexual and apomictic gametophytes of *C. thalictroides* [22]. In parallel to glycolysis, the pentose phosphate pathway generates NADPH and pentoses. This metabolic pathway is represented in our dataset by the proteins 6-PHOSPHOGLUCONATE DEHYDROGENASE, 1 DECARBOXYLATING 1 (PGD1), GLUCOSE-6-PHOSPHATE 1-DEHYDROGENASE 6 (G6PD6), and PHOSPHOGLYCERATE KINASE 1 (PGK1). Specifically, a mutation in the gene of the first protein may decrease cellulose synthesis, thus altering the structure and composition of the primary cell wall [38]. The enzyme G6PD6 is important for the synthesis of fatty acids and nucleic acids involved in membrane synthesis and cell division [39]. G6PD6 was also reported in the vegetative tissues of the lycophyte *S. tamariscina*, which was involved in the response to drought [11], and the protein PGD1 was identified by analyzing stipe explants of the fern *C. delgadii*, and found to be associated with direct somatic embryogenesis [19].

Metabolism of lipids

Regarding the metabolism of lipids, three proteins were identified in this study. The first protein is ENOYL-[ACYL-CARRIER-PROTEIN] REDUCTASE (MOD1), which catalyzes the last reduction step of the de novo fatty acid synthesis cycle and the fatty acid elongation cycle. A mutation causing a decreased activity of this protein reduces the number of fatty acids, which triggers mosaic premature cell death and changes in the plant's

morphology, such as chlorotic and curly leaves, distorted siliques, and dwarfism [40]. The second protein is ATP-CITRATE SYNTHASE ALPHA CHAIN PROTEIN 1 (ACLA-1), which is necessary for the normal growth and development of plants because it synthesizes acetyl-CoA, a key compound for many metabolic pathways (fatty acids and glucosinolates in chloroplasts; flavonoids, sterols, and phospholipids in the cytoplasm; and ATP and amino acid carbon skeletons in mitochondria). Moreover, it is the substrate for histone acetylation in the nucleus, affecting chromosome structure and regulating transcription [41,42]. The third protein is CITRATE SYNTHASE 2 (CSY2), which synthesizes citrate in peroxisomes for the respiration of fatty acids in seedlings and is required for seed germination [43].

Biosynthesis of amino acids and nucleotides

Involved in the biosynthesis of amino acids, we found the proteins ASPARTATE AMINOTRANSFERASE (ASP1); 3-ISOPROPYLMALATE DEHYDRATASE LARGE SUBUNIT (IIL1), which acts in glucosinolate biosynthesis involved in the defense against insects [44]; FERREDOXIN-DEPENDENT GLUTAMATE SYNTHASE 1 (GLU1), which is required for the re-assimilation of ammonium ions generated during photorespiration [45]; HISTIDINOL DEHYDROGENASE (HISN8); and S-ADENOSYLMETHIONINE SYNTHASE 4 (METK4) [46–48]. We also identified proteins associated with the metabolism of nucleotides, specifically with AMP syntheses, such as ADENOSINE KINASE 1 (ADK1) and ADENYLOSUCCINATE SYNTHETASE (PURA). Of note is the protein PROBABLE RIBOSE-5-PHOSPHATE ISOMERASE 3 (RPI3), which is essential for the synthesis of numerous compounds such as purines, pyrimidines, aromatic amino acids, NAD, and NADP [38]. Apart from the proteins mentioned above, we found some that are associated with the biosynthesis of nucleotide sugars, such as the two pyrophosphorylases GLUCOSE-1-PHOSPHATE ADENYLYLTRANSFERASE SMALL SUBUNIT (ADG1) and GLUCOSE-1-PHOSPHATE ADENYLYLTRANSFERASE LARGE SUBUNIT 1 (ADG2).

Metabolism of energy

The protein OXYGEN-EVOLVING ENHANCER PROTEIN 1-2 (PSBO2), which regulates the replacement of the protein D1 impaired by light [49], and the protein THYLAKOID LUMENAL 16.5 kDa were reported. The latter protein is necessary to carry out photosynthesis correctly and efficiently under two conditions: controlled photoinhibitory light and fluctuating light. In nature, plants experience rapid and extreme changes in sunlight, requiring rapid adaptation [50]. Involved in photosynthesis, we found the protein PHOTOSYNTHETIC NDH SUBUNIT OF LUMENAL LOCATION 5 (PNLS5), which modulates the conformation of the protein BRASSINAZOLE-RESISTANT 1 (BZR1) [51]. This protein binds to the promoter of the gene *FLOWERING LOCUS D* (*FLD*) and represses its expression, eventually leading to the expression of the *FLOWERING LOCUS C* (*FLC*) gene, which encodes a repressor of flowering [51]. Finally, CBBY-LIKE PROTEIN (CBBY) degrades xylulose-1,5-bisphosphate, a potent inhibitor of the protein RUBISCO [52]. On the other hand, photorespiration represents a waste of the energy produced by photosynthesis. The enzyme D-GLYCERATE 3-KINASE (GLYK) catalyzes the final reaction of photorespiration [53]. Another important protein for photorespiration is SERINE-GLYOXYLATE AMINOTRANSFERASE (AGT1), which also participates in primary and lateral root development [54]. The latter protein was also reported in the fern *C. delgadii* [19].

Sulfur and nitrogen metabolism

Proteins involved in sulfur metabolism are represented by UDP-SULFOQUINOVOSE SYNTHASE (SQD1), which converts UDP-glucose and sulfite to the precursor of the main group of sulfolipids, UDP-sulfoquinovose, thus preventing sulfite from accumulating as it is toxic to the cell [55], and SUFE-LIKE PROTEIN 1 (SUFE1), a sulfur acceptor that activates cysteine desulfurases in plastids and mitochondria, which is essential for embryogenesis [56]. Regarding nitrogen metabolism, there are the proteins NITROGEN REGULATORY PROTEIN P-II HOMOLOG (GLB1), which is a nitrogen regulatory protein and intervenes in glycosaminoglycan degradation [57], and FERREDOXIN-NITRITE REDUCTASE (NIR1), which catalyzes the reduction of nitrite to ammonium [58]. As the amount of this protein in

the cell increases, the tolerance and assimilation of nitrogen dioxide by the plant improves. As nitrogen dioxide is an air pollutant produced largely by motorized vehicles, plants could act as a sink for this substance, i.e., this protein could be used in biotechnological applications for bioremediation [58].

Metabolism of secondary compounds

Several proteins related to flavonoid biosynthesis are represented in this work, such as CHALCONE-FLAVANONE ISOMERASE 1 (CHI1), which is responsible for the isomerization of chalcones into naringenin [59]. We also found enzymes involved in the biosynthesis of terpenoids, such as HETERODIMERIC GERANYLGERANYL PYROPHOSPHATE SYNTHASE LARGE SUBUNIT 1 (GGPPS1); the biosynthesis of lignans, PHENYLCOUMARAN BENZYLIC ETHER REDUCTASE 1 (PCBER1); and the biosynthesis of phenylpropanoids. We also found the protein 4-COUMARATE-COA LIGASE 3 (4CL3), which produces CoA-thioesters of hydroxy- and methoxy-substituted cinnamic acids, used to synthesize anthocyanins, flavonoids, isoflavonoids, coumarins, lignin, suberin, and phenols [60], and 3-PHOSPHOSHIKIMATE 1-CARBOXYVINYLTRANSFERASE (AT2G45300), involved in the synthesis of chorismate, which is the precursor of the amino acids phenylalanine, tryptophan, and tyrosine [61]. The proteins 4CL3 and the transferases GLUTATHIONE S-TRANSFERASE L2 (GSTL2) and GLUTATHIONE S-TRANSFERASE L3 (GSTL3) found in our species, was also studied in the fern *A. spinulosa* [29]. The last ones catalyze the glutathione-dependent reduction of S-glutathionyl quercetin to quercetin [62]. Besides, GSTL2 and GSTL3 proteins were also reported in a lycophyte, *S. tamariscina*, where they are required in the response to desiccation [11].

3.2. Genetic Information Processing

Transcription and translation

In the gametophytes of *D. affinis* and *D. oreades*, we identified two proteins involved in transcription, specifically the 14-3-3-like proteins 14-3-3-LIKE PROTEIN GF14 NU (GRF7) and 14-3-3-LIKE PROTEIN GF14 IOTA (GRF12), which are associated with a DNA-binding complex that binds to the G-box, a cis-regulatory DNA element [63]. These 14-3-3-like proteins were also studied in two species: the lycophyte *S. tamariscina* [11] and the fern *C. delgadii* [19]. Related to translation, we found GLYCINE-RICH RNA-BINDING PROTEIN 3 (RBG3), which has a role in RNA processing during stress, specifically in editing cytosine to uracil in mitochondrial RNA, thereby controlling 6% of all mitochondrial editing sites [64]. This protein was also identified in *S. tamariscina* when studying the response to drought [11], as well as other proteins, such as PUTATIVE PENTATRICOPEPTIDE REPEAT-CONTAINING PROTEIN AT1G03510 (PCMP-E3), POLYADENYLATE-BINDING PROTEIN RBP47B (RBP47B), and UBP1-ASSOCIATED PROTEIN 2A (UBA2A), which regulates mRNAs and stabilizes RNAs in the nucleus [65]. Apart from several ribosomal subunits, there are others linked to translation elongation, like the protein ELONGATION FACTOR 2 (LOS1), which is also involved in the response to cold [66].

Protein folding and sorting

Once the proteins have been formed, there is a quality check to ensure that they have been synthesized completely and folded correctly. Among the proteins playing a major role in the acceleration of folding or the degradation of misfolded proteins are CHAPERONIN 1 (CPN10-1) and PEPTIDYL-PROLYL CIS-TRANS ISOMERASE FKBP16-4 (FKBP16-4). The gametophyte of the ferns under study harbor proteins linked to the sorting or transport of molecules within the cell and between the inside and outside of cells. In line with this, we found PROTEIN TRANSLOCASE SUBUNIT SECA1 (SECA1), which has a role in coupling ATP hydrolysis to protein transfer across the thylakoid membrane, thus participating in photosynthetic acclimation and chloroplast formation [67]; IMPORTIN SUBUNIT ALPHA-2 (IMPA2), which acts in nuclear import [68]; the proteins ADP and ATP CARRIER (AAC2), which mediates the import of ADP into the mitochondrial matrix [69], and TIC62 (TIC62), which is involved in the import of nuclear-encoded proteins into

chloroplasts [70]. The IMPA-2 protein was also identified when studying germinating spores of the fern *O. cinnamomea* [4]. In addition, we found proteins associated with the transport of water and small hydrophilic molecules through the cell membrane: PROBABLE AQUAPORIN PIP1-4 (PIP1.4) [71]. COATOMER SUBUNIT ALPHA-1 (AT1G62020) and COATOMER SUBUNIT GAMMA (AT4G34450) are associated with clathrin-uncoated vesicles that are transported from the endoplasmic reticulum to the Golgi apparatus and vice versa. In contrast, the proteins CLATHRIN INTERACTOR EPSIN 2 (EPSIN2) and DYNAMIN-2B (DRP2B) are related to clathrin-coated vesicles, with the latter participating in planar polarity formation to correctly positioning the root hairs [72].

Protein degradation

Among the proteases, we found ATP-DEPENDENT CLP PROTEASE PROTEOLYTIC SUBUNIT-RELATED PROTEIN 3 (CLPR3) and ATP-DEPENDENT CLP PROTEASE ATP-BINDING SUBUNIT CLPT2 (CLPR2). Plants need to cope with heat stress, and for this, the gametophytes studied here rely on the aminopeptidases LEUCINE AMINOPEPTIDASE 1 and LEUCINE AMINOPEPTIDASE 3 (LAP1 and LAP3), which are probably involved in the processing and turnover of intracellular proteins and function as molecular chaperones protecting proteins from heat-induced damage [73].

3.3. Protein–Protein Interactions

Using the STRING platform, we thoroughly analyzed—one by one—the interactions of the groups of proteins studied. We observed that for the metabolism of carbohydrates, evidence from co-expression, text mining, and experiments were stronger between the mitochondrial proteins SUCCINATE-CoA LIGASE [ADP-FORMING] SUBUNIT BETA and SUBUNIT ALPHA-1 than the others in this group. Both proteins are involved in the tricarboxylic acid cycle [74].

Among the proteins for biosynthesis of amino acids, evidence from co-expression was stronger between the proteins ASPARTATE-SEMIALDEHYDE DEHYDROGENASE and DIHYDROXY-ACID DEHYDRATASE (DHAD), while evidence from databases was stronger between DIHYDROXY-ACID DEHYDRATASE and 2-ISOPROPYLMALATE SYNTHASE 2 (IPMS2), 3-ISOPROPYLMALATE DEHYDRATASE LARGE SUBUNIT (IIL1) and 2-ISOPROPYLMALATE SYNTHASE 2, and 3-ISOPROPYLMALATE DEHYDRATASE LARGE SUBUNIT and 3-ISOPROPYLMALATE DEHYDROGENASE 2 (IMD2). In fact, these proteins are involved in the synthesis of numerous compounds necessary for plant growth and development: ASPARTATE-SEMIALDEHYDE DEHYDROGENASE for the biosynthesis of lysine, threonine, and methionine [75]; DIHYDROXY-ACID DEHYDRATASE for isoleucine and valine [76]; 2-ISOPROPYLMALATE SYNTHASE 2 and 3-ISOPROPYLMALATE DEHYDROGENASE 2 for leucine [77,78]; and 3-ISOPROPYLMALATE DEHYDRATASE LARGE SUBUNIT for glucosinolates [44].

For the metabolism of energy, evidence from co-expression was stronger between the proteins ATP SYNTHASE GAMMA CHAIN 1 (ATPC1) and GLYCERALDEHYDE-3-PHOSPHATE DEHYDROGENASE (GAPA-2), while experimental data provided strong evidence for the interaction between PHOTOSYSTEM I P700 CHLOROPHYLL A APOPROTEIN A1 (PSAA) and PHOTOSYSTEM I IRON-SULFUR CENTER (PSAC). In photosynthesis, the C-terminus of PSAC interacts with PSAA and other proteins, such as PHOTOSYSTEM I P700 CHLOROPHYLL A APOPROTEIN A2 (PSAB) and PHOTOSYSTEM I REACTION CENTER SUBUNIT II-1 (PSAD1), for its assembly into the photosystem I [79]. Evidence from databases indicated an interaction between SERINE-GLYOXYLATE AMINOTRANSFERASE (*AGT1*) and GLYCOLATE OXIDASE 2 (GLO2), both proteins being involved in photorespiration [54], while evidence from text mining suggested an interaction between OXYGEN-EVOLVING ENHANCER PROTEIN 1-2 (PSBO2) and OXYGEN-EVOLVING ENHANCER PROTEIN 2-1 (PSBP1), both being chloroplastic oxygen-evolving enhancer proteins that form part of photosystem II [49].

For the metabolism of secondary compounds, evidence from text mining was the strongest, indicating an interaction between PHENYLALANINE AMMONIA-LYASE 1

(PAL1) and PHENYLALANINE AMMONIA-LYASE 4 (PAL4). Both proteins participate in the synthesis from phenylalanine of numerous compounds based on the phenylpropane skeleton, which is fundamental to plant metabolism [80].

With respect to transcription and translation, co-expression evidence was stronger between ribosomal proteins.

Finally, for protein transport, co-expression data provided the strongest evidence for interactions between the proteins COATOMER SUBUNIT ALPHA-1 and COATOMER SUBUNIT GAMMA; experimental data for the interaction between COATOMER SUBUNIT ALPHA-1 and COATOMER SUBUNIT DELTA; and text mining data for the interactions between PROTEIN TRANSLOCASE SUBUNIT SECA1 and ATPase GET3B.

As indicated in the results, in the group related to the metabolism of carbohydrates, the protein with the most interactions was PHOSPHOGLYCERATE KINASE 1, which is involved in glycolysis [81]. For the biosynthesis of amino acids, ASPARTATE-SEMIALDEHYDE DEHYDROGENASE, DIHYDROXY-ACID DEHYDRATASE, and 3-ISOPROPYLMALATE DEHYDROGENASE 2 were involved in several biosynthetic pathways: lysine, leucine, valine, isoleucine, methionine, and threonine [77]. In the group metabolism of energy, ATP SYNTHASE GAMMA CHAIN 1 had the highest number of interactions, likely because it is part of a chloroplastic ATP synthase [82]. The protein 4-COUMARATE-COA LIGASE 3 had the most interactions in the group metabolism of secondary compounds. It plays a key role in the synthesis of numerous secondary metabolites, such as anthocyanins, flavonoids, isoflavonoids, coumarins, lignin, suberin, and phenols [60]. In transcription and translation, the ribosomal proteins LARGE RIBOSOMAL SUBUNIT PROTEIN UL4Z, SMALL RIBOSOMAL SUBUNIT PROTEIN US11X, and SMALL RIBOSOMAL SUBUNIT PROTEIN US17Y, which are necessary for the formation of ribosomes, had the highest number of interactions [83]. Finally, in transport, the proteins PROTEIN TRANSLOCASE SUBUNIT SECA1 and COATOMER SUBUNIT GAMMA participate in coupling ATP hydrolysis to protein transfer across the thylakoid membrane and in the transport of clathrin-uncoated vesicles from the endoplasmic reticulum to the Golgi apparatus and vice versa, respectively [67].

Regarding the statistical analysis of the two highest scoring types of interactions in the studied groups of metabolism of carbohydrates (database and text mining) and transcription and translation (experiments and co-expression), Pearson's correlation coefficients, which measure the tendency of two vectors to increase or decrease together, were significant. One of the most popular types of data in databases is text, and the process of synthesizing information is known as text mining. In the case of proteins linked to carbohydrate metabolism, there seems to be a lot of information in databases about it, and therefore text mining could be enriched as well. Regarding transcription and translation, we speculate that most of the experiments on molecular biology cope with these processes, reporting more genes involved on them.

4. Materials and Methods

4.1. Plant Material and Growth Conditions

Spores of *D. affinis* were obtained from sporophytes growing in Turón valley (Asturias, Spain), 477 m a.s.l., 43°12'10" N–5°43'43" W. For *D. oreades*, spores were collected from sporophytes growing in Neila lagoons (Burgos, Spain), 1.920 m a.s.l., 42°02'48" N–3°03'44" W. Spores were released from sporangia, soaked in water for 2 h, and then washed for 10 min with a solution of NaClO (0.5%) and Tween 20 (0.1%). Then, they were rinsed three times with sterile, distilled water. Spores were centrifuged at 1300 × *g* for 3 min between rinses and then cultured in 500 mL Erlenmeyer flasks containing 100 mL of liquid Murashige and Skoog (MS) medium [84]. Unless otherwise noted, media were supplemented with 2% sucrose (*w/v*), and the pH was adjusted to 5.7 with 1 or 0.1 N NaOH. The cultures were kept on an orbital shaker (75 rpm) at 25 °C under cool, white fluorescent light (70 μmol m⁻²s⁻¹) with a 16 h photoperiod.

Following spore germination, filamentous gametophytes were subcultured into 200 mL flasks containing 25 mL of MS medium supplemented with 2% sucrose (*w/v*) and 0.7% agar. The gametophytes of *D. affinis* became two-dimensional, arriving at the spatulate and heart stage after 20 or 30 additional days, respectively. Gametophytes of *D. oreades* grew slower and needed around six months to become cordate and reach sexual maturity (Figure 5). Apomictic and sexual gametophytes were collected, and images were taken under a light microscope (Nikon Eclipse E600, Tokyo, Japan) using microphotographic equipment (DS Camera Control, Nikon, Tokyo, Japan). Gametophytes of *D. oreades* had only female reproductive organs (i.e., archegonia), while cordate, apomictic gametophytes of *D. affinis* had visible developing apogamic centers composed of smaller and darker isodiametric cells. Samples of apomictic and sexual cordate gametophytes were weighed before and after lyophilization for 48 h (Telstar-Cryodos, Terrassa, Spain) and stored in Eppendorf tubes in a freezer at $-20\text{ }^{\circ}\text{C}$ until use.

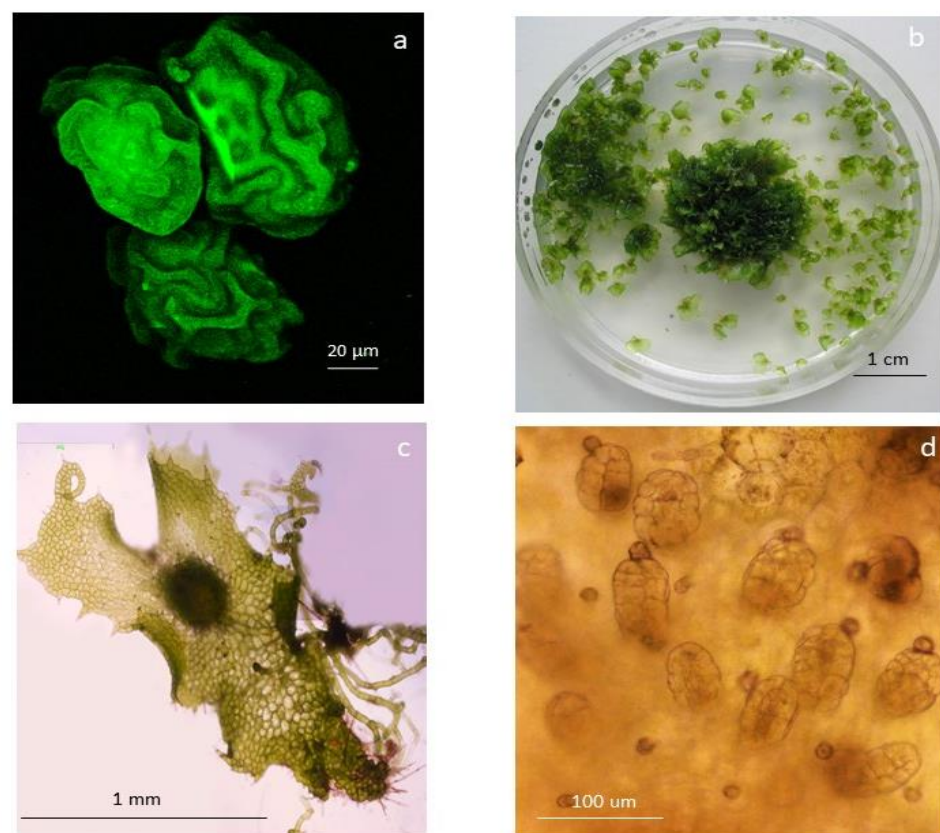


Figure 5. Morphological traits in the apomictic fern *D. affinis* and its sexual relative *D. oreades*: (a) confocal image of spores of *D. affinis*; (b) gametophytes of *D. affinis* growing in a Petri dish; (c) image taken under a light microscope of a cordate gametophyte of *D. affinis* showing an apogamic center in the middle; and (d) archegonia in the gametophyte of *D. oreades*.

4.2. Protein Extraction, Separation, and In-Gel Digestion

The present work expands previous bioinformatic analyses, and, specifically, it is carried out with a set of 218 proteins, which had been extracted and annotated as follows.

The protocol used for protein extraction, separation, and in-gel digestion was reported earlier [31]. In brief, samples were solubilized with 800 μL of buffer A (0.5 M Tris-HCl (pH 8.0), 5 mM EDTA, 0.1 M HEPES-KOH, 4 mM DTT, 15 mM EGTA, 1 mM PMSF, 0.5% (*w/v*) PVP, and 1x protease inhibitor cocktail (Roche, Rotkreuz, Switzerland)) and homogenized, and proteins were extracted in two steps: first, the homogenate was subjected to centrifugation at $16,200\times g$ for 10 min at $4\text{ }^{\circ}\text{C}$ on a tabletop centrifuge, and, second, the supernatant was subjected to ultracentrifugation at 117–124 kPa ($100,000\times g$) for 45 min at

4 °C in an Airfuge (Beckman Coulter, Pasadena, CA, USA), yielding the soluble protein fraction in the supernatant. In parallel, the pellet obtained from the first ultracentrifugation was re-dissolved in 200 µL of buffer B (40 mM Tris-base, 40 mM DTT, 4% (*w/v*) SDS, and 1× protease inhibitor cocktail (Roche, Rotkreuz, Switzerland)) to extract membrane proteins using the ultracentrifuge, as described above, in the supernatant. Protein concentrations were determined using a Qubit Fluorometer (Invitrogen, Carlsbad, CA, USA), and 1D gel electrophoresis was performed as follows: 1 mg protein was treated with sample loading buffer and 2 M DTT, heated at 99 °C for 5 min, followed by a short cooling period on ice, and then loaded separately onto a 0.75 mm thick, 12% SDS-PAGE mini-gel. Electrophoresis conditions were 150 V and 250 mA for 1 h in 1× running buffer.

4.3. Protein Separation and In-Gel Digestion

Each gel lane was cut into six 0.4 cm wide sections resulting in 48 slices, and then fragmented into smaller pieces and subjected to 10 mM DTT (in 25 mM AmBic, pH8) for 45 min at 56 °C and 50 mM iodoacetamide for 1 h at room temperature in the dark prior to trypsin digestion at 37 °C overnight. Subsequently, gel pieces were washed twice with 100 µL of 100 mM NH₄HCO₃/50% acetonitrile and washed once with 50 µL acetonitrile. At this point, the supernatants were discarded. Peptides were digested with 20 µL trypsin (5 ng/L in 10 mM Tris/2 mM CaCl₂, pH 8.2) and 50 µL buffer (10 mM Tris/2 mM CaCl₂, pH 8.2). After microwave-heating for 30 min at 60 °C, the supernatant was removed, and gel pieces were extracted once with 150 µL 0.1% TFA/50% acetonitrile. All supernatants were put together, then dried and dissolved in 15 µL 0.1% formic acid/3% acetonitrile, and, finally, transferred to auto-sampler vials for liquid chromatography (LC)-tandem mass spectrometry (MS/MS) for which 5 µL was injected.

4.4. Protein Identification, Verification, and Bioinformatic Downstream Analyses

MS/MS and peptide identification (Orbitrap XL) were performed according to [31]. Scaffold software (version Scaffold 4.2.1, Proteome Software Inc., Portland, OR, USA) was used to validate MS/MS-based peptide and protein identifications. Mascot results were analyzed together using the MudPIT option. Peptide identifications were accepted if they scored better than 95.0% probability as specified by the Peptide Prophet algorithm with delta mass correction, and protein identifications were accepted if the Protein Prophet probability was above 95%. Indeed, the unique peptide $\geq 2'$ was considered. Proteins that contained the same peptides and could not be differentiated based on MS/MS alone were grouped to satisfy the principles of parsimony using the scaffolds cluster analysis option. Only proteins that met the above criteria were considered as positively identified for further analysis. The number of random matches was evaluated by performing the Mascot searches against a database containing decoy entries and checking how many decoy entries (proteins or peptides) passed the applied quality filters. The peptide FDR and protein FDR were estimated at 2% and 1%, respectively, indicating the stringency of the analyses. A semi-quantitative spectrum counting analysis was conducted. The “total spectrum count” for each protein and each sample was reported, and these spectrum counts were averaged for each species, *D. affinis* and *D. oreades*. Then, one “1” was added to each average in order to prevent division by zero, and a log₂ ratio of the averaged spectral counts from *D. affinis* versus *D. oreades* was calculated. Proteins were considered as differentially expressed if this log₂ ratio was above 0.99. This refers to at least twice as many peptide spectrum match (PSM) assignments in one group compared to the other. Also, to provide some functional understanding of the identified proteins, we blasted the whole protein sequences of all identified proteins against *Sellginella moellendorffii* and *A. thaliana* Uniprot sequences and retrieved the best matching identifier from each of them along with the corresponding e-value, accepting blast-hits with values below 1×10^{-7} . These better-described ortholog identifiers were then used in further downstream analysis.

4.5. Protein Analysis Using the STRING Platform

The identifiers of the genes from apomictic and sexual gametophyte samples were used as input for STRING platform version 11.5 analysis, and a high threshold (0.700) was selected for a positive interaction between a pair of proteins.

4.6. Statistical Analyses

Regarding the two major protein–protein interactions highlighted for carbohydrate metabolism, amino acid biosynthesis, energy metabolism, and transcription and translation, a Pearson’s correlation test was performed using R software 4.2.0, and *p*-values lower than 0.05 were considered significant.

5. Conclusions

The analysis of a set of 218 proteins shared by the gametophytes of the apomictic fern *D. affinis* and its sexual relative *D. oreades* revealed the presence of proteins mostly involved in biological functions associated with metabolism, the processing of genetic information, and abiotic stresses. Some smaller protein groups were studied in detail: metabolism of carbohydrates; biosynthesis of amino acids; metabolism of energy; metabolism of secondary compounds; transcription, translation, and transport; and abiotic stress. Possible interactions between these proteins were identified, with the most common source of evidence for interactions stemming from databases and information from text mining. The proteins involved in transcription and translation exhibit the strongest interactions. The description of possible biological functions and the possible protein–protein interactions among the identified proteins expands our current knowledge about ferns and plants in general.

Supplementary Materials: The supporting information can be downloaded at <https://www.mdpi.com/article/10.3390/ijms241512429/s1>.

Author Contributions: Conceptualization, H.F. and U.G.; methodology, H.F., J.G., V.G., J.M.A. and S.O.; formal analysis, J.G. and H.F.; writing—original draft preparation, H.F. and S.O., with help from U.G.; writing—review and editing, U.G., J.G., V.G., L.G.Q. and J.M.A.; funding acquisition, H.F. and U.G.; resources, L.G.Q. and U.G. All authors have read and agreed to the published version of the manuscript.

Funding: This research was supported by core funding of the University of Zurich to U.G., the University of Oviedo through the Grant CESSTT1819 for the International Mobility of Research Staff to H.F., and the European Union’s 7th Framework Program: PRIME-XS-000252 to H.F. and U.G.

Institutional Review Board Statement: Not applicable.

Informed Consent Statement: Not applicable.

Data Availability Statement: The concatenated dDB is available online at http://fgcz-r-021.uzh.ch/fasta/p1222_combo_NGS_n_Viridi_20160205.fasta (accessed on 9 November 2022).

Acknowledgments: We thank the University of Oviedo for a grant from the International Mobility of Research Staff, according to the collaboration agreement CESSTT1819, and the Functional Genomics Center Zurich for access to its excellent infrastructure. We also thank Hanspeter Schöb for his logistic support during H.F.’s visits to the Grossniklaus laboratory.

Conflicts of Interest: The authors declare no conflict of interest.

References

1. Wada, M. The fern as a model system to study photomorphogenesis. *J. Plant Res.* **2007**, *120*, 3–16. [[CrossRef](#)]
2. Salmi, M.L.; Bushart, T.; Stout, S.; Roux, S. Profile and analysis of gene expression changes during early development in germinating spores of *Ceratopteris richardii*. *Plant Physiol.* **2005**, *138*, 1734–1745. [[CrossRef](#)] [[PubMed](#)]
3. Salmi, M.L.; Morris, K.E.; Roux, S.J.; Porterfield, D.M. Nitric oxide and CGMP signaling in calcium-dependent development of cell polarity in *Ceratopteris richardii*. *Plant Physiol.* **2007**, *144*, 94–104. [[CrossRef](#)] [[PubMed](#)]
4. Suo, J.; Zhao, Q.; Zhang, Z.; Chen, S.; Cao, J.; Liu, G.; Wei, X.; Wang, T.; Yang, C.; Dai, S. Cytological and proteomic analyses of *Osmunda cinnamomea* germinating spores reveal characteristics of fern spore germination and rhizoid tip growth. *Mol. Cell. Proteom.* **2015**, *14*, 2510–2534. [[CrossRef](#)]

5. Salmi, M.L.; Bushart, T.J. Cellular, molecular, and genetic changes during the development of *Ceratopteris richardii* gametophytes. In *Working with Ferns: Issues and Applications*; Fernández, H., Kumar, A., Revilla, M.A., Eds.; Springer International Publishing: New York, NY, USA, 2010; pp. 11–24.
6. Eeckhout, S.; Leroux, O.; Willats, W.G.; Popper, Z.A.; Viane, R.L. Comparative glycan profiling of *Ceratopteris richardii* ‘C-fern’ gametophytes and sporophytes links cell-wall composition to functional specialization. *Ann. Bot.* **2014**, *114*, 1295–1307. [[CrossRef](#)] [[PubMed](#)]
7. Fernández, H.; Revilla, M.A. In vitro culture of ornamental ferns. *Plant Cell. Tissue Organ Cult.* **2003**, *73*, 1–13. [[CrossRef](#)]
8. Rivera, A.; Cañal, M.J.; Grossniklaus, U.; Fernández, H. The gametophyte of fern: Born to reproduce. In *Current Advances in Fern Research*; Fernández, H., Ed.; Springer International Publishing: New York, NY, USA, 2018; pp. 3–19.
9. Chen, C.-Y.; Chiu, F.-Y.; Lin, Y.; Huang, W.-J.; Hsieh, P.-S.; Hsu, F.-L. Chemical constituents analysis and antidiabetic activity validation of four fern species from Taiwan. *Int. J. Mol. Sci.* **2015**, *16*, 2497–2516. [[CrossRef](#)]
10. Femi-Adepoju, A.G.; Dada, A.O.; Otun, K.O.; Adepoju, A.O.; Fatoba, O.P. Green synthesis of silver nanoparticles using terrestrial fern (*Gleichenia pectinata* (Willd.) C. Presl.): Characterization and antimicrobial studies. *Heliyon* **2019**, *5*, e01543. [[CrossRef](#)]
11. Wang, X.; Chen, S.; Zhang, H.; Shi, L.; Cao, F.; Guo, L.; Xie, Y.; Wang, T.; Yan, X.; Dai, S. Desiccation tolerance mechanism in resurrection fern-ally *Selaginella tamariscina* revealed by physiological and proteomic analysis. *J. Proteome Res.* **2010**, *9*, 6561–6577. [[CrossRef](#)]
12. Rathinasabapathi, B. Ferns represent an untapped biodiversity for improving crops for environmental stress tolerance. *New Phytol.* **2006**, *172*, 385–390. [[CrossRef](#)]
13. Dhir, B. Role of ferns in environmental cleanup. In *Current Advances in Fern Research*; Fernández, H., Ed.; Springer International Publishing: Cham, Switzerland, 2018; pp. 517–531.
14. Barker, M.S.; Wolf, P.G. Unfurling fern biology in the genomics age. *Bioscience* **2010**, *60*, 177–185. [[CrossRef](#)]
15. Der, J.P.; Barker, M.S.; Wickett, N.J.; de Pamphilis, C.W.; Wolf, P.G. De novo characterization of the gametophyte transcriptome in bracken fern, *Pteridium aquilinum*. *BMC Genom.* **2011**, *12*, 99. [[CrossRef](#)] [[PubMed](#)]
16. Bona, E.; Marsano, F.; Massa, N.; Cattaneo, C. Proteomic analysis as a tool for investigating arsenic stress in *Pteris vittata* roots colonized or not by arbuscular mycorrhizal symbiosis. *J. Proteom.* **2011**, *74*, 1338–1350. [[CrossRef](#)]
17. Valledor, L.; Menéndez, V.; Canal, M.J.; Revilla, A.; Fernández, H. Proteomic approaches to sexual development mediated by antheridiogen in the fern *Blechnum spicant* L. *Proteomics* **2014**, *14*, 2061–2071. [[CrossRef](#)] [[PubMed](#)]
18. Aya, K.; Kobayashi, M.; Tanaka, J.; Ohyanagi, H.; Suzuki, T.; Yano, K.; Takano, T.; Yano, K.; Matsuoka, M. De novo transcriptome assembly of a fern, *Lygodium japonicum*, and a web resource database Ljtrans DB. *Plant Cell Physiol.* **2015**, *56*, e5. [[CrossRef](#)]
19. Domzalska, L.; Kędracka-Krok, S.; Jankowska, U.; Grzyb, M.; Sobczak, M.; Rybczyński, J.J.; Mikula, A. Proteomic analysis of stipe explants reveals differentially expressed proteins involved in early direct somatic embryogenesis of the tree fern *Cyathea delgadii* Sternb. *Plant Sci.* **2017**, *258*, 61–76. [[CrossRef](#)] [[PubMed](#)]
20. Sigel, E.M.; Schuettpehl, E.; Pryer, K.M.; Der, J.P. Overlapping patterns of gene expression between gametophyte and sporophyte phases in the fern *Polypodium amorphum* (Polypodiales). *Front. Plant Sci.* **2018**, *9*, 1450. [[CrossRef](#)]
21. Sareen, B.; Thapa, P.; Joshi, R.; Bhattacharya, A. Proteome analysis of the gametophytes of a western Himalayan fern *Diplazium maximum* reveals their adaptive responses to changes in their micro-environment. *Front. Plant Sci.* **2019**, *10*, 1623. [[CrossRef](#)]
22. Chen, X.; Chen, Z.; Huang, W.; Fu, H.; Wang, Q.; Wang, Y.; Cao, J. Proteomic analysis of gametophytic sex expression in the fern *Ceratopteris thalictroides*. *PLoS ONE* **2019**, *14*, e0221470. [[CrossRef](#)]
23. Fu, Q.; Chen, L. Comparative transcriptome analysis of two reproductive modes in *Adiantum reniforme* var. *sinense* targeted to explore possible mechanism of apogamy. *BMC Genet.* **2019**, *20*, 1–14. [[CrossRef](#)]
24. Cordle, A.; Irish, E.; Cheng, C.L. Gene expression associated with apogamy commitment in *Ceratopteris richardii*. *Sex. Plant Reprod.* **2012**, *25*, 293–304. [[CrossRef](#)] [[PubMed](#)]
25. Atallah, N.M.; Vitek, O.; Gaiti, F.; Tanurdzic, M.; Banks, J.A. Sex determination in *Ceratopteris richardii* is accompanied by transcriptome changes that drive epigenetic reprogramming of the young gametophyte. *G3* **2018**, *8*, 2205–2214. [[CrossRef](#)] [[PubMed](#)]
26. Youngstrom, C.E.; Geadelmann, L.F.; Irish, E.E.; Cheng, C.-L. A fern *WUSCHEL-RELATED HOMEBOX* gene functions in both gametophyte and sporophyte generations. *BMC Plant Biol.* **2019**, *19*, 1–13. [[CrossRef](#)] [[PubMed](#)]
27. Aragón-Raygoza, A.; Herrera-Estrella, L.; Cruz-Ramirez, A. Transcriptional analysis of *Ceratopteris richardii* young sporophyte reveals conservation of stem cell factors in the root apical meristem. *Front. Plant Sci.* **2022**, *13*, 924660. [[CrossRef](#)]
28. Hong, Y.; Wang, Z.; Li, M.; Su, Y.; Wang, T. First multi-organ full-length transcriptome of tree fern *Alsophila spinulosa* highlights the stress-resistant and light-adapted genes. *Front. Plant Sci.* **2022**, *12*, 784546. [[CrossRef](#)]
29. Huang, X.; Wang, W.; Gong, T.; Wickell, D.; Kuo, L.-Y.; Zhang, X.; Wen, J.; Kim, H.; Lu, F.; Zhao, H.; et al. The flying spider-monkey tree fern genome provides insights into fern evolution and arborescence. *Nat. Plants* **2022**, *8*, 500–512. [[CrossRef](#)]
30. Xia, Z.; Liu, L.; Wei, Z.; Wang, F.; Shen, H.; Yan, Y. Analysis of comparative transcriptome and positively selected genes reveal adaptive evolution in leaf-less and root-less whisk ferns. *Plants* **2022**, *11*, 1198. [[CrossRef](#)]
31. Grossmann, J.; Fernández, H.; Chaubey, P.M.; Valdés, A.E.; Gagliardini, V.; Cañal, M.J.; Russo, G.; Grossniklaus, U. Proteogenomic analysis greatly expands the identification of proteins related to reproduction in the apogamous fern *Dryopteris affinis* ssp. *affinis*. *Front. Plant Sci.* **2017**, *8*, 336. [[CrossRef](#)]

32. Wyder, S.; Rivera, A.; Valdés, A.E.; Cañal, M.J.; Gagliardini, V.; Fernández, H.; Grossniklaus, U. Differential gene expression profiling of one- and two-dimensional apogamous gametophytes of the fern *Dryopteris affinis* ssp. *affinis*. *Plant Physiol. Biochem.* **2020**, *148*, 302–311. [[CrossRef](#)]
33. Fernández, H.; Grossmann, J.; Gagliardini, V.; Feito, I.; Rivera, A.; Rodríguez, L.; Quintanilla, L.G.; Quesada, V.; Cañal, M.J.; Grossniklaus, U. Sexual and apogamous species of woodferns show different protein and phytohormone profiles. *Front. Plant Sci.* **2021**, *12*, 718932. [[CrossRef](#)]
34. Ojosnegros, S.; Alvarez, J.M.; Grossmann, J.; Gagliardini, V.; Quintanilla, L.G.; Grossniklaus, U.; Fernández, H. The shared proteome of the apomictic fern *Dryopteris affinis* ssp. *affinis* and its sexual relative *Dryopteris oreades*. *Int. J. Mol. Sci.* **2022**, *23*, 14027. [[CrossRef](#)]
35. Tronconi, M.A.; Fahnenstich, H.; Gerrard Weehler, M.C.; Andreo, C.S.; Flügge, U.I.; Drincovich, M.F.; Maurino, V.G. *Arabidopsis* NAD-malic enzyme functions as a homodimer and heterodimer and has a major impact on nocturnal metabolism. *Plant Physiol.* **2008**, *146*, 1540. [[CrossRef](#)]
36. Zhao, Z.; Assmann, S.M. The glycolytic enzyme, phosphoglycerate mutase, has critical roles in stomatal movement, vegetative growth, and pollen production in *Arabidopsis thaliana*. *J. Exp. Bot.* **2011**, *62*, 5179. [[CrossRef](#)] [[PubMed](#)]
37. Tomaz, T.; Bagard, M.; Pracharoenwattana, I.; Lindén, P.; Lee, C.P.; Carroll, A.J.; Ströher, E.; Smith, S.M.; Gardeström, P.; Millar, A.H. Mitochondrial malate dehydrogenase lowers leaf respiration and alters photorespiration and plant growth in *Arabidopsis*. *Plant Physiol.* **2010**, *154*, 1143–1157. [[CrossRef](#)] [[PubMed](#)]
38. Howles, P.A.; Birch, R.J.; Collings, D.A.; Gebbie, L.K.; Hurley, U.A.; Hocart, C.H.; Arioli, T.; Williamson, R.E. A mutation in an *Arabidopsis* ribose 5-phosphate isomerase reduces cellulose synthesis and is rescued by exogenous uridine. *Plant J.* **2006**, *48*, 606–618. [[CrossRef](#)]
39. Wakao, S.; Benning, C. Genome-wide analysis of glucose-6-phosphate dehydrogenases in *Arabidopsis*. *Plant J.* **2005**, *41*, 243–256. [[CrossRef](#)] [[PubMed](#)]
40. Mou, Z.; He, Y.; Dai, Y.; Liu, X.; Li, J. Deficiency in fatty acid synthase leads to premature cell death and dramatic alterations in plant morphology. *Plant Cell* **2000**, *12*, 405–417. [[CrossRef](#)]
41. Fatland, B.L.; Ke, J.; Anderson, M.D.; Mentzen, W.L.; Wei Cui, L.; Christy Allred, C.; Johnston, J.L.; Nikolau, B.J.; Syrkin Wurtele, E.; Biology LWC, M. Molecular characterization of a heteromeric ATP-citrate lyase that generates cytosolic acetyl-coenzyme A in *Arabidopsis*. *Plant Physiol.* **2002**, *130*, 740–756. [[CrossRef](#)]
42. Fatland, B.L.; Nikolau, B.J.; Wurtele, E.S. Reverse genetic characterization of cytosolic acetyl-CoA generation by ATP-citrate lyase in *Arabidopsis*. *Plant Cell* **2005**, *17*, 182–203. [[CrossRef](#)] [[PubMed](#)]
43. Pracharoenwattana, I.; Cornah, J.E.; Smith, S.M. *Arabidopsis* peroxisomal citrate synthase is required for fatty acid respiration and seed germination. *Plant Cell* **2005**, *17*, 2037–2048. [[CrossRef](#)]
44. Knill, T.; Reichelt, M.; Paetz, C.; Gershenzon, J.; Binder, S. *Arabidopsis thaliana* encodes a bacterial-type heterodimeric isopropyl-malate isomerase involved in both Leu biosynthesis and the Met chain elongation pathway of glucosinolate formation. *Plant Mol. Biol.* **2009**, *71*, 227–239. [[CrossRef](#)]
45. Ishizaki, T.; Ohsumi, C.; Totsuka, K.; Igarashi, D. Analysis of glutamate homeostasis by overexpression of Fd-GOGAT gene in *Arabidopsis thaliana*. *Amin. Acids* **2009**, *38*, 943–950. [[CrossRef](#)] [[PubMed](#)]
46. Zhang, Y.; Sun, K.; Sandoval, F.J.; Santiago, K.; Roje, S. One-carbon metabolism in plants: Characterization of a plastid serine hydroxymethyltransferase. *Biochem. J.* **2010**, *430*, 97–105. [[CrossRef](#)] [[PubMed](#)]
47. Petersen, L.N.; Marineo, S.; Mandalà, S.; Davids, F.; Sewell, B.T.; Ingle, R.A. The missing link in plant histidine biosynthesis: *Arabidopsis* MYOINOSITOL MONOPHOSPHATASE-LIKE2 encodes a functional histidinol-phosphate phosphatase. *Plant Physiol.* **2010**, *152*, 1186–1196. [[CrossRef](#)] [[PubMed](#)]
48. Shen, B.; Li, C.; Tarczynski, M.C. High free-methionine and decreased lignin content result from a mutation in the *Arabidopsis* S-ADENOSYL-L-METHIONINE SYNTHETASE 3 gene. *Plant J.* **2002**, *29*, 371–380. [[CrossRef](#)] [[PubMed](#)]
49. Lundin, B.; Hansson, M.; Schoefs, B.; Vener, A.V.; Spetea, C. The *Arabidopsis* PsbO2 protein regulates dephosphorylation and turnover of the photosystem II reaction centre D1 protein. *Plant J.* **2007**, *49*, 528–539. [[CrossRef](#)] [[PubMed](#)]
50. Liu, J.; Last, R.L. A chloroplast thylakoid lumen protein is required for proper photosynthetic acclimation of plants under fluctuating light environments. *Proc. Natl. Acad. Sci. USA* **2017**, *114*, E8110–E8117. [[CrossRef](#)]
51. Zhang, Y.; Li, B.; Xu, Y.; Li, H.; Li, S.; Zhang, D.; Mao, Z.; Guo, S.; Yang, C.; Weng, Y.; et al. The cyclophilin CYP20-2 modulates the conformation of BRASSINAZOLE-RESISTANT1, which binds the promoter of *FLOWERING LOCUS D* to regulate flowering in *Arabidopsis*. *Plant Cell* **2013**, *25*, 2504–2521. [[CrossRef](#)]
52. Bracher, A.; Sharma, A.; Starling-Windhof, A.; Hartl, F.U.; Hayer-Hartl, M. Degradation of potent RUBISCO inhibitor by selective sugar phosphatase. *Nat. Plants* **2014**, *112015*, 1–7. [[CrossRef](#)]
53. Boldt, R.; Edner, C.; Kolukisaoglu, Ü.; Hagemann, M.; Weckwerth, W.; Wienkoop, S.; Morgenthal, K.; Bauwe, H. D-glycerate 3-kinase, the last unknown enzyme in the photorespiratory cycle in *Arabidopsis*, belongs to a novel kinase family. *Plant Cell* **2005**, *17*, 2413–2420. [[CrossRef](#)]
54. Wang, R.; Yang, L.; Han, X.; Zhao, Y.; Zhao, L.; Xiang, B.; Zhu, Y.; Bai, Y.; Wang, Y. Overexpression of AtAGT1 promoted root growth and development during seedling establishment. *Plant Cell Rep.* **2019**, *38*, 1165–1180. [[CrossRef](#)] [[PubMed](#)]
55. Sanda, S.; Leustek, T.; Theisen, M.J.; Garavito, R.M.; Benning, C. Recombinant *Arabidopsis* SQD1 converts UDP-glucose and sulfite to the sulfolipid head group precursor UDP-sulfoquinovose in vitro. *J. Biol. Chem.* **2001**, *276*, 3941–3946. [[CrossRef](#)] [[PubMed](#)]

56. Ye, H.; Abdel-Ghany, S.E.; Anderson, T.D.; Pilon-Smits, E.A.; Pilon, M. CpSufE activates the cysteine desulfurase CpNifS for chloroplastic Fe-S cluster formation. *J. Biol. Chem.* **2006**, *281*, 8958–8969. [[CrossRef](#)] [[PubMed](#)]
57. Ferrario-Méry, S.; Meyer, C.; Hodges, M. Chloroplast nitrite uptake is enhanced in *Arabidopsis* PII mutants. *FEBS Lett.* **2008**, *582*, 1061–1066. [[CrossRef](#)]
58. Takahashi, M.; Sasaki, Y.; Ida, S.; Morikawa, H. Nitrite reductase gene enrichment improves assimilation of NO₂ in *Arabidopsis*. *Plant Physiol.* **2001**, *126*, 731–741. [[CrossRef](#)]
59. Shirley, B.W.; Hanley, S.; Goodman, H.M. Effects of ionizing radiation on a plant genome: Analysis of two *Arabidopsis* transparent *testa* mutations. *Plant Cell* **1992**, *4*, 333–347. [[CrossRef](#)]
60. Ehlting, J.; Büttner, D.; Wang, Q.; Douglas, C.J.; Somssich, I.E.; Kombrink, E. Three 4-coumarate: Coenzyme A ligases in *Arabidopsis thaliana* represent two evolutionarily divergent classes in angiosperms. *Plant J.* **1999**, *19*, 9–20. [[CrossRef](#)]
61. Klee, H.J.; Muskopf, Y.M.; Gasser, C.S. Cloning of an *Arabidopsis thaliana* gene encoding 5-enolpyruvyl shikimate-3-phosphate synthase: Sequence analysis and manipulation to obtain glyphosate-tolerant plants. *Mol. Gen. Genet.* **1987**, *210*, 437–442. [[CrossRef](#)]
62. Dixon, D.P.; Edwards, R. Roles for stress-inducible lambda glutathione transferases in flavonoid metabolism in plants as identified by ligand fishing. *J. Biol. Chem.* **2010**, *285*, 36322–36329. [[CrossRef](#)]
63. Rosenquist, M.; Alsterfjord, M.; Larsson, C.; Sommarin, M. Data mining the *Arabidopsis* genome reveals fifteen 14-3-3 genes: Expression is demonstrated for two out of five novel genes. *Plant Physiol.* **2001**, *127*, 142–149. [[CrossRef](#)]
64. Shi, X.; Hanson, M.R.; Bentolila, S. Two RNA recognition motif-containing proteins are plant mitochondrial editing factors. *Nucleic Acids Res.* **2015**, *43*, 3814–3825. [[CrossRef](#)]
65. Lambermon, M.H.L.; Fu, Y.; Kirk, D.A.W.; Dupasquier, M.; Filipowicz, W.; Lorković, Z.J. UBA1 and UBA2, two proteins that interact with UBP1, a multifunctional effector of pre-mRNA maturation in plants. *Mol. Cell. Biol.* **2002**, *22*, 4346–4357. [[CrossRef](#)] [[PubMed](#)]
66. Guo, Y.; Xiong, L.; Ishitani, M.; Zhu, J.K. An *Arabidopsis* mutation in TRANSLATION ELONGATION FACTOR 2 causes superinduction of CBF/DREB1 transcription factor genes but blocks the induction of their downstream targets under low temperatures. *Proc. Natl. Acad. Sci. USA* **2002**, *99*, 7786–7791. [[CrossRef](#)]
67. Skalitzky, C.A.; Martin, J.R.; Harwood, J.H.; Beirne, J.J.; Adamczyk, B.J.; Heck, G.R.; Cline, K.; Fernandez, D.E. Plastids contain a second Sec translocase system with essential functions. *Plant Physiol.* **2011**, *155*, 354–369. [[CrossRef](#)] [[PubMed](#)]
68. Bhattacharjee, S.; Lee, L.Y.; Oltmanns, H.; Cao, H.; Veena; Cuperus, J.; Gelvin, S.B. IMPa-4, an *Arabidopsis* importin α isoform, is preferentially involved in *Agrobacterium*-mediated plant transformation. *Plant Cell* **2008**, *20*, 2661–2680. [[CrossRef](#)]
69. Haferkamp, I.; Hackstein, J.H.P.; Voncken, F.G.J.; Schmit, G.; Tjaden, J. Functional integration of mitochondrial and hydrogenosomal ADP/ATP carriers in the *Escherichia coli* membrane reveals different biochemical characteristics for plants, mammals and anaerobic chytrids. *Eur. J. Biochem.* **2002**, *269*, 3172–3181. [[CrossRef](#)]
70. Küchler, M.; Decker, S.; Hörmann, F.; Soll, J.; Heins, L. Protein import into chloroplasts involves redox-regulated proteins. *EMBO J.* **2002**, *21*, 6136–6145. [[CrossRef](#)]
71. Lee, S.H.; Chung, G.C.; Jang, J.Y.; Ahn, S.J.; Zwiazek, J.J. Overexpression of PIP2;5 aquaporin alleviates effects of low root temperature on cell hydraulic conductivity and growth in *Arabidopsis*. *Plant Physiol.* **2012**, *159*, 479–488. [[CrossRef](#)]
72. Stanislas, T.; Hüser, A.; Barbosa, I.C.R.; Kiefer, C.S.; Brackmann, K.; Pietra, S.; Gustavsson, A.; Zourelidou, M.; Schwechheimer, C.; Grebe, M. *Arabidopsis* D6PK is a lipid domain-dependent mediator of root epidermal planar polarity. *Nat. Plants* **2015**, *1*, 15162. [[CrossRef](#)] [[PubMed](#)]
73. Scranton, M.A.; Yee, A.; Park, S.Y.; Walling, L.L. Plant leucine aminopeptidases moonlight as molecular chaperones to alleviate stress-induced damage. *J. Biol. Chem.* **2012**, *287*, 18408–18417. [[CrossRef](#)]
74. Tan, Y.-F.; O'Toole, N.; Taylor, N.L.; Millar, A.H. Divalent metal ions in plant mitochondria and their role in interactions with proteins and oxidative stress-induced damage to respiratory function. *Plant Physiol.* **2010**, *152*, 747–761. [[CrossRef](#)]
75. Zhang, Y.; Swart, C.; Alseekh, S.; Scossa, F.; Jiang, L.; Obata, T.; Graf, A.; Fernie, A.R. The extra-pathway interactome of the TCA cycle: Expected and unexpected metabolic interactions. *Plant Physiol.* **2018**, *177*, 966–979. [[CrossRef](#)]
76. Yan, Y.; Liu, Q.; Zang, X.; Yuan, S.; Bat-Erdene, U.; Nguyen, C.; Gan, J.; Zhou, J.; Jacobsen, S.E.; Tang, Y. Resistance-gene-directed discovery of a natural-product herbicide with a new mode of action. *Nature* **2018**, *559*, 415–418. [[CrossRef](#)]
77. de Kraker, J.W.; Luck, K.; Textor, S.; Tokuhisa, J.G.; Gershenzon, J. Two *Arabidopsis* genes (*IPMS1* and *IPMS2*) encode isopropylmalate synthase, the branchpoint step in the biosynthesis of leucine. *Plant Physiol.* **2007**, *143*, 970–986. [[CrossRef](#)] [[PubMed](#)]
78. He, Y.; Chen, L.; Zhou, Y.; Mawhinney, T.P.; Chen, B.; Kang, B.H.; Hauser, B.A.; Chen, S. Functional characterization of *Arabidopsis thaliana* isopropylmalate dehydrogenases reveals their important roles in gametophyte development. *New Phytol.* **2011**, *189*, 160–175. [[CrossRef](#)]
79. Varotto, C.; Pesaresi, P.; Meurer, J.; Oelmüller, R.; Steiner-Lange, S.; Salamini, F.; Leister, D. Disruption of the *Arabidopsis* photosystem I gene *psaE1* affects photosynthesis and impairs growth. *Plant J.* **2000**, *22*, 115–124. [[CrossRef](#)]
80. Cochrane, F.C.; Davin, L.B.; Lewis, N.G. The *Arabidopsis* phenylalanine ammonia lyase gene family: Kinetic characterization of the four PAL isoforms. *Phytochemistry* **2004**, *65*, 1557–1564. [[CrossRef](#)]
81. Gargano, D.; Maple-Groedem, J.; Moeller, S.G. In vivo phosphorylation of FtsZ2 in *Arabidopsis thaliana*. *Biochem. J.* **2012**, *446*, 517–521. [[CrossRef](#)]

82. Takagi, D.; Amako, K.; Hashiguchi, M.; Fukaki, H.; Ishizaki, K.; Goh, T.; Fukao, Y.; Sano, R.; Kurata, T.; Demura, T.; et al. Chloroplastic ATP synthase builds up a proton motive force preventing production of reactive oxygen species in photosystem I. *Plant J.* **2017**, *91*, 306–324. [[CrossRef](#)] [[PubMed](#)]
83. Carroll, A.J.; Heazlewood, J.L.; Ito, J.; Millar, A.H. Analysis of the *Arabidopsis* cytosolic ribosome proteome provides detailed insights into its components and their post-translational modification. *Mol. Cell Proteom.* **2008**, *7*, 347–369. [[CrossRef](#)] [[PubMed](#)]
84. Murashige, T.; Skoog, F. A revised medium for rapid growth and bioassays with tobacco tissue cultures. *Plant Physiol.* **1962**, *15*, 473–497. [[CrossRef](#)]

Disclaimer/Publisher’s Note: The statements, opinions and data contained in all publications are solely those of the individual author(s) and contributor(s) and not of MDPI and/or the editor(s). MDPI and/or the editor(s) disclaim responsibility for any injury to people or property resulting from any ideas, methods, instructions or products referred to in the content.